SYNTHETIC APERTURE RADAR SIGNALS: FORMULATIONS AND APPROACHES FOR DATA ANALYSIS

Antonio B. Lucero, et al

Technology Service Corporation

Prepared for:

Office of Naval Research

May 1975

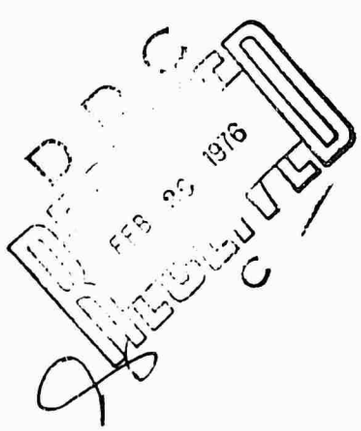

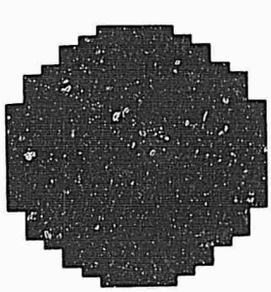

Technology Service Corporation

Technology Service Corporation
2811 Wilshire Boulevard
Santa Monica, California 90403
(213)829-7411

SYNTHETIC APERTURE RADAR SIGNALS:

FORMULATIONS AND APPROACHES

TSC-PD-134-2

May 1975

by

Antonio B. Lucero
Peter Swerling
Leo Breiman

With Contributions From:

Glenn A. Gray
William S. Meisel
Fred E. Nathanson
Michael R. O'Sullivan

Submitted to: Mathematical and Information
Sciences Division
Office of Naval Research
Arlington, Virginia

SECURITY CLASSIFICATION OF THIS PAGE (When Data Entered)

REPORT DOCUMENTATION PAGE		READ INSTRUCTIONS BEFORE COMPLETING FORM
1. REPORT NUMBER	2. GOVT ACCESSION NO.	3. RECIPIENT'S CATALOG NUMBER
4. TITLE (and Subtitle) Synthetic Aperture Radar Signals Formulations and Approaches for Data Analysis		5. TYPE OF REPORT & PERIOD COVERED Final 6. PERFORMING ORG. REPORT NUMBER TSC-PD-134-2*
7. AUTHOR(s) A. B. Lucero P. Swerling L. Breiman		8. CONTRACT OR GRANT NUMBER(s) N00014-75-C-0088
9. PERFORMING ORGANIZATION NAME AND ADDRESS Technology Service Corporation 2811 Wilshire Boulevard Santa Monica, Calif. 90403		10. PROGRAM ELEMENT, PROJECT, TASK AREA & WORK UNIT NUMBERS
11. CONTROLLING OFFICE NAME AND ADDRESS Mathematical and Information Sciences Division Office of Naval Research Arlington, Virginia 22217		12. REPORT DATE May 1975* 13. NUMBER OF PAGES 134
14. MONITORING AGENCY NAME & ADDRESS (if different from Controlling Office)		15. SECURITY CLASS. (of this report) Unclassified 15a. DECLASSIFICATION/DOWNGRADING SCHEDULE

16. DISTRIBUTION STATEMENT (of this Report)

Approved for public release; distribution unlimited

17. DISTRIBUTION STATEMENT (of the abstract entered in Block 20, if different from Report)

18. SUPPLEMENTARY NOTES

*This report supersedes and replaces TSC-PD-134-1 dated 24 November 1974

19. KEY WORDS (Continue on reverse side if necessary and identify by block number)

Synthetic Aperture Radar
Radar Imagery
Imagery Analysis
Statistical Analysis of Radar Imagery
Statistical Models of Radar Targets

20. ABSTRACT (Continue on reverse side if necessary and identify by block number)

Discusses principles of synthetic aperture radar, properties of radar targets, characteristics of radar imagery, statistical analysis of radar imagery, and the application of modern data analysis.

DD FORM 1 JAN 73 1473 EDITION OF 1 NOV 65 IS OBSOLETE

SECURITY CLASSIFICATION OF THIS PAGE (When Data Entered)

FOREWORD

This report was sponsored by the Office of Naval Research, Mathematical and Information Sciences Division. It presents an introduction to the subject of synthetic aperture radar which is intended to serve as a vehicle to help statisticians and data analysts define topics for future research. These areas of future research are intended to center around the processing of synthetic aperture radar (SAR) data, especially with respect to image interpretation and radar target signature analysis.

Some specific objectives of this paper are (1) to produce a document containing background information and a fundamental discussion of the nature of SAR signals, error sources, phase history correlation, and the status of SAR hardware; (2) to produce a document that is intelligible to mathematicians and statisticians who are unfamiliar with the specialized SAR terminology; and (3) to identify potential areas for exploitation by data analysts and statisticians.

The principal author of this report is Mr. Antonio B. Lucero of Technology Service Corporation (TSC), 2811 Wilshire Boulevard, Santa Monica, California 90403. He was assisted in the preparation of some of the material by Dr. Peter Swerling, Dr. Leo Breiman, and other members of the TSC staff.

The work was performed in support of Contract N0014-75-C-0088 (ONR Identifying Number NR 048-625) "Synthetic Aperture Radar Signals: Formulations and Approaches."

ABSTRACT

This paper provides an introduction to the principles of synthetic aperture radar. It discusses the elements of radar signals, radar measurements, and radar systems analysis. Based on these fundamentals, the concepts and operation of synthetic aperture radar are presented. Then the properties of radar targets and their radar returns are discussed. The principle of frequency diversity to obtain independent samples is also introduced. Synthetic aperture imagery characteristics are explained and examples presented. A variety of approaches to imagery interpretation and target signature analysis are discussed. Statistical theories and data analysis approaches are presented along with recommended areas for further study by statisticians.

TABLE OF CONTENTS

LIST OF FIGURES

LIST OF FIGURES (Cont'd)

1.0 INTRODUCTION

Modern synthetic aperture radar (SAR) systems are currently presenting vast quantities of data from which information must be extracted that is relevant to a particular mission. These data may consist of optically processed radar images composed of millions of resolution cells. Or, after detection and isolation of a radar target, the data may consist of only a few thousand resolution cells. In either case, the data to be processed and analyzed consist of a large number of observables, each of which may have its own independent probability distribution.

It is therefore clear that automatic or semiautomatic techniques for processing and analyzing SAR data would be desirable. The generic types of problems in which statisticians and data-analysts could assist should include, but not be limited to, formulation of statistical models, abstracting concrete problems into objective mathematical formulations of hypotheses, and testing of hypotheses for applications such as detection of spatial or temporal changes, location of transition boundaries, and classification or identification of radar targets.

However, before addressing such potential problems for statisticians and data analysts, it is important for such researchers to have an appreciation for SAR data, SAR systems, radar targets, and imagery characteristics, as well as previous statistical work in this area.

1.1 Preliminaries

The main body of this report is concerned with providing background material on radar fundamentals (Section 1.0), synthetic aperture systems

(Section 2.0), radar targets (Section 3.0), imagery characteristics (Section 4.0), and imagery interpretation and signature analysis (Section 5.0). A detailed discussion on categories of statistical fluctuation models and the use of scattering mechanisms in model postulation have been adapted from Dr. Peter Swerling's Lecture Notes and are included in Appendices B and C.

The approach that has been taken in this report is to start from basic physics fundamentals, assuming that those readers who are familiar with physics concepts would necessarily include readers who are also familiar with concepts in electrical engineering. Only the essentials of each major topic are presented; thus, each concept is presented in only one way. This is somewhat different from the usual approach taken in radar literature, where, for example, a process may be explained both in the time domain and in the frequency domain. It was felt that the subject, being unfamiliar to the intended readers, would become confusing with alternate interpretations rather than a single interpretation.

One result of this approach has been that the discussion on processing of SAR signals has been limited to optical processing. To avoid giving the reader the false impression that only optical processing is employed, it is useful, at the outset, to point out that (1) optical processing is the usual way in which SAR images are formed, (2) digital/electronic SAR processing systems are currently being used in experimental prototype systems, (3) most future systems will tend to be digital, and (4) digital systems have many advantages over optical systems (e.g., real-time processing and display and instant control over image quality).

However, if the reader has grasped the material in this report, he will understand most of the underlying concepts in all types of SAR data,

especially the output imagery data. Basically, the only differences of output data are format and sampling rate - the digital output may be displayed on a cathode ray tube (a television type of device), whereas the optically processed output is usually on film. The lower sampling rate of digital displays produces a somewhat different characteristic on the fine structure of the imagery, which causes the images to appear as a collection of, more or less, symmetrical blobs. The optically processed images, on the other hand, are composed of non-symmetrical blobs with a great variety of shapes ("the can of worms effect"). The information content in both cases, however, is the same.

1.2 Radar Fundamentals

In order to gain a comprehensive understanding of synthetic aperture radar data, it is necessary to understand certain fundamental properties of radars, radar targets, and the basic information that is available from radars.

Electromagnetic Waves

Radars operate by radiating electromagnetic energy and collecting the energy reflected back by objects. The radiated energy is in the form of electromagnetic waves whose wavelengths may be as long as 100 meters for some radars or as short as 10^{-5} meters for other radars. In principle, these electromagnetic waves can be generated by electrons oscillating at frequencies as low as 3×10^{6} cycles per second for a wavelength of 10^{2} meters and as high as 3×10^{13} cycles per second for a wavelength of 10^{-5} meters. In practice, however, frequencies as low as 3×10^{7} cycles per second (Hertz) and as high as 3×10^{10} Hertz are commonly used.

The relationship between wavelength λ and frequency f is given by the equation

$$c = f\lambda \quad , \tag{1}$$

where c is a constant, namely, the speed of light in free space which is equal to 2.99774×10^8 meters/second.

Radar Signals

The electromagnetic signals emanating from such an oscillator operating at a frequency f would vary with time t as

$$S(t) = A\cos(2\pi ft) \quad , \tag{2}$$

where A is a constant. A more general form allowing for amplitude modulation and phase (or frequency) modulation is

$$S(t) = a(t)\cos[2\pi f_o t + \phi(t)] \quad , \tag{3}$$

where a(t) defines the oscillation amplitude as a function of time, and f_o is the nominal or "carrier" frequency of the signal and $\phi(t)$ is a generalized phase modulation function. The instantaneous frequency f_i can be found from

$$2\pi f_i t = 2\pi f_o t + \phi(t) \tag{4a}$$

and

$$\frac{d(2\pi f_i t)}{dt} = \frac{d(2\pi f_o t + \phi(t))}{dt} \quad . \tag{4b}$$

Thus, in general,

$$f_i = f_o + \frac{1}{2\pi}\frac{d\phi(t)}{dt} \quad . \tag{5}$$

Radar Antennas

Analogous to the ordinary flashlight reflector, radars employ antennas to concentrate the radiated (or received) power in a given direction. Antennas may take any one of a wide variety of forms. One common form is the parabolic dish reflector, shown in Figure 1. As suggested by this figure, energy concentrated at the antenna feed (as in the case of a flashlight bulb) is radiated toward the reflecting surface. The reflecting surface, in turn, causes the direction of propagation of the emanating rays to become parallel and the resultant signal to be in phase across the beam. At sufficiently distant range from the radar, the distribution of energy as a function of elevation and azimuth angles is shown in Figure 2. This is the diffraction pattern imposed by the size and shape of the antenna aperture. Since most radars cannot distinguish, for example, two small reflecting objects that lie within the main lobe of the radiation pattern from a single strong reflector, the resolving ability of an antenna is estimated by the width of its main lobe. The width of the main lobe at one-half

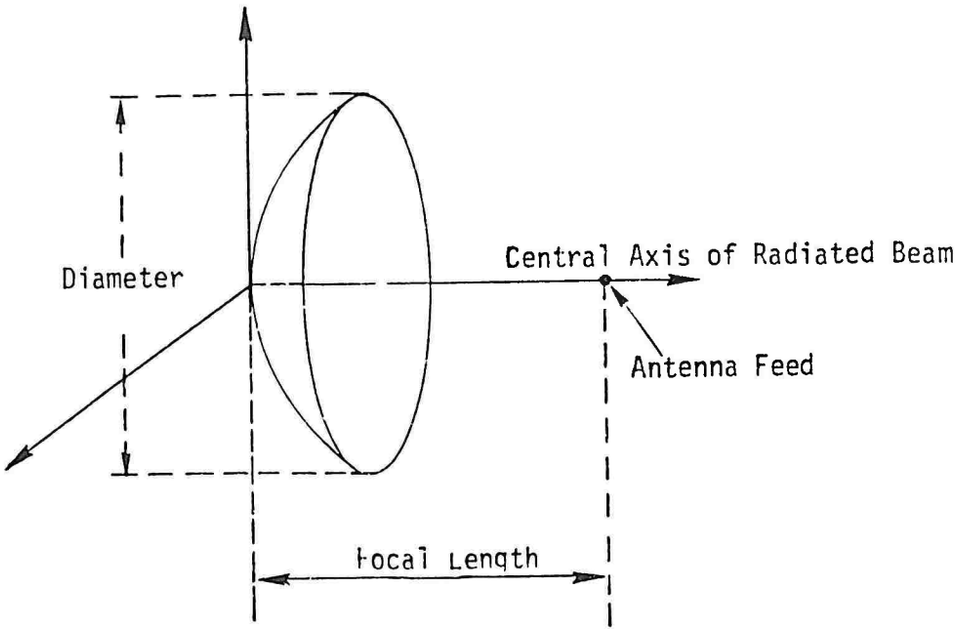

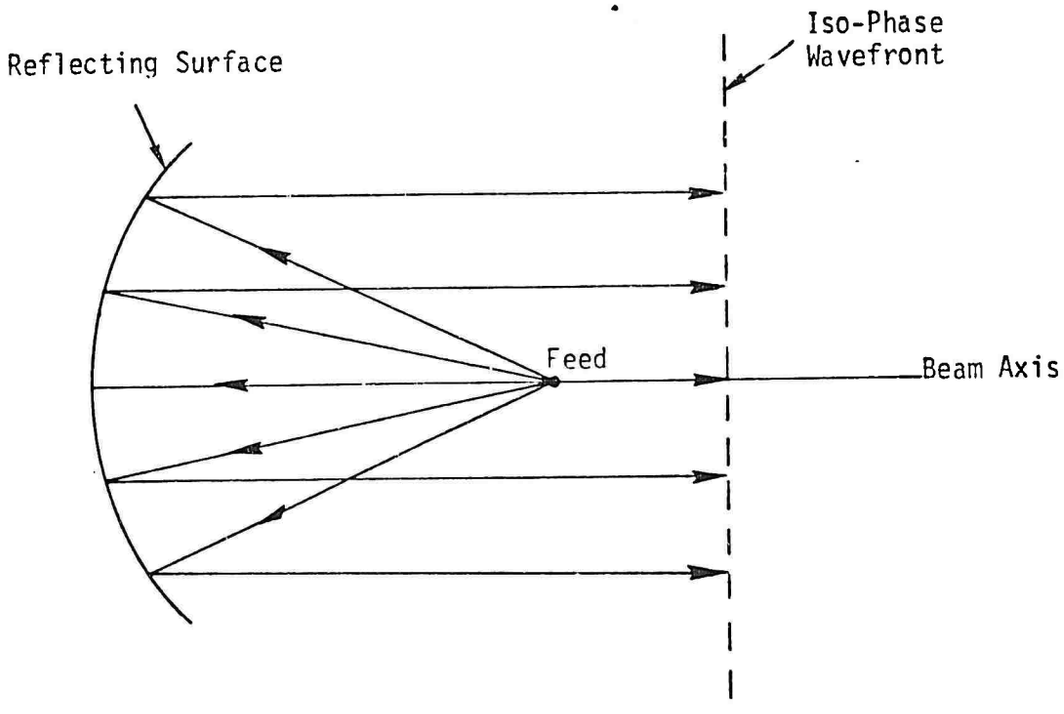

Figure 1. Parabolic Dish Antenna
(Adapted from Reference 1.)

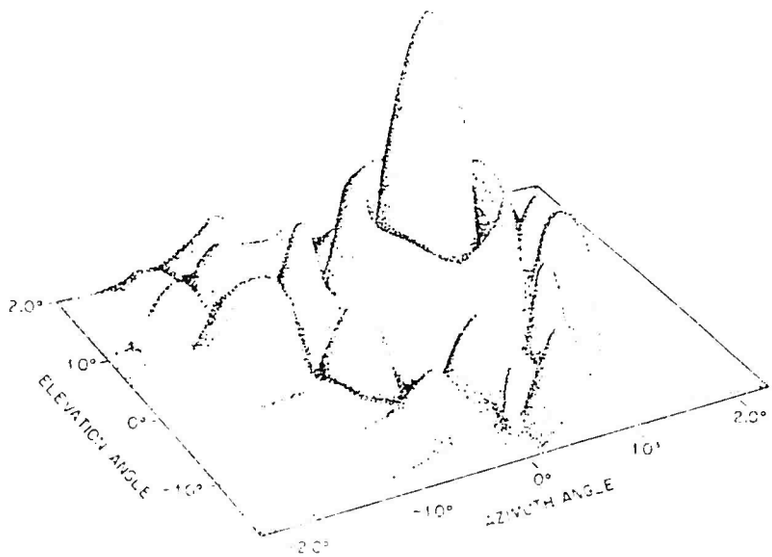

Figure 2. Typical Antenna Radiation Pattern

(Reference 1.)

the peak radiation intensity is usually the resolution that is referenced. In Figure 2, if the vertical scale were linear, then the resolution of this antenna would be about 10° in elevation and azimuth.

Another common form of antenna is the linear array. In this case the antenna is made up of a number of radiating elements (e.g., simple dipole antennas) placed at regular intervals along a straight line. To operate this type of antenna, signals are fed simultaneously to each of the antenna elements for transmission. Likewise, when used as a receiver, the elements receive radar returns simultaneously. By use of time delays and weighting functions internal to the radar system, addition of the signals between the elements, in both amplitude and phase, is exploited to steer and shape the energy distribution (the radiation pattern of the antenna beam).

If the radiating elements are identical, then the net radiation pattern in a plane containing the array has a half-power width of

$$\beta = \frac{\lambda}{L} \quad \text{(radians)}, \tag{6}$$

where L is the length of the linear array.

Compared to a radar without an antenna, the increase in power density for the linear array antenna is approximately L/λ; for the parabolic dish antenna the increase is about $4\pi A/\lambda$, where A is the area of the dish.

1.3 Radar Measurements

A wide range of measurements can be performed with a radar, depending upon its built-in capabilities, the operating environment, and the signal processing employed. Below are presented the fundamental radar measurements that can be performed and how these fundamental measurements can be used to estimate radar target properties.

Range Measurement

By measuring the delay in time τ between the transmission of an electromagnetic signal and its received "echo", the range R to an object can be determined from the equation

$$R = c\tau/2 \quad , \tag{7}$$

based upon the fact that electromagnetic waves travel at the speed of light. The factor of 2 in Equation (7) accounts for the path length to and from the object.

Doppler Measurement

When there is sufficient relative motion between an object and a radar, an effect known as a doppler frequency shift takes place. By way of illustration, Figure 3 depicts the geometrical arrangement of a moving radar, a stationary reflecting object, and the flight vector of the radar platform. Let v be the magnitude of the flight vector; λ the wavelength transmitted by the radar; and $90° - \theta$ the angle between the flight vector and the radar line-of-sight to the object. Then the doppler shift ν is given by

$$\nu = 2v/\lambda \sin \theta \quad . \tag{8}$$

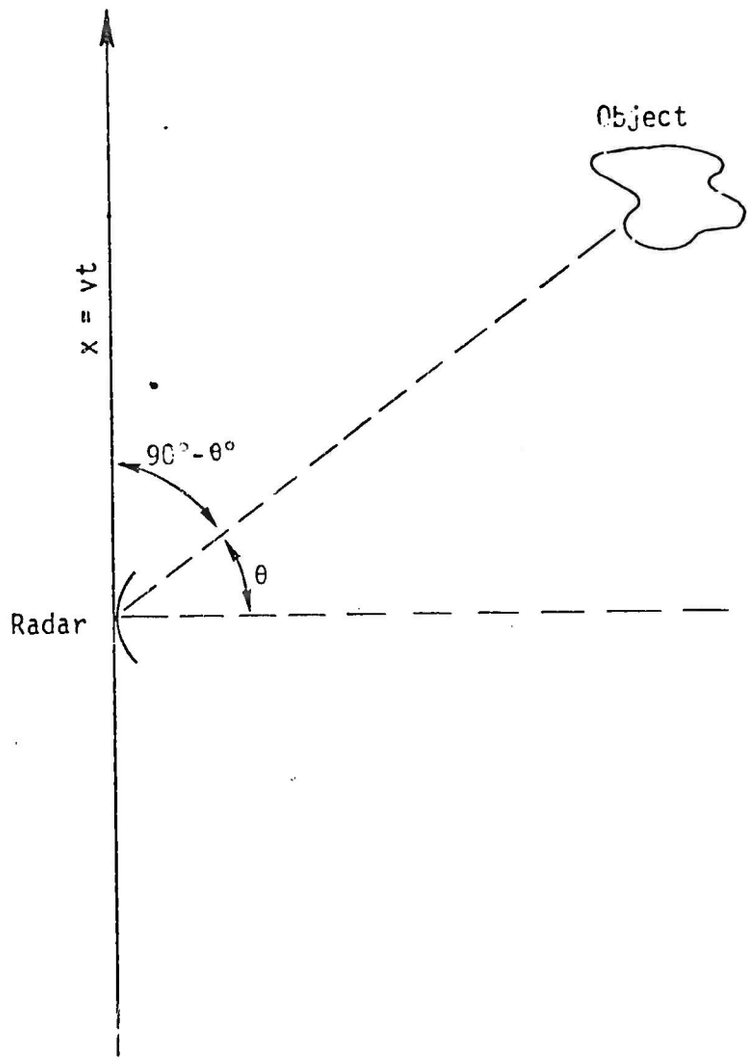

Figure 3. Illustration of Geometrical Arrangement of Moving Radar and a Stationary Reflecting Object

Thus, if the radar were transmitting at a frequency f, the echo from this object would be at another frequency $f' = f + \nu$. At an early point in time $f' > f$; when the line-of-sight is perpendicular to the flight vector and sin $\theta = 0$, the doppler shift is zero and $f' = f$; and at a later point in time $f' < f$.

The doppler frequency ν could be estimated from the received signal as follows. If the transmitted signal is as shown in Equation (2), then the received signal S_R would have the same form, except for the amplitude A_R and time delay τ

$$S_R(t) = A_R \cos [2\pi f_o(t-\tau)] \quad . \tag{9}$$

As the radar platform moves, the range to the object changes; and, consequently, the delay is also a function of time. Thus, Equation (9) may be rewritten as in Equation (3), where the phase modulation

$$\phi(t) = -2\pi f_o \tau(t) \quad . \tag{10}$$

As a result, the instantaneous frequency f_i as given by Equation (5)

$$f_i = f_o\left(1 - \frac{d\tau}{dt}\right) \quad . \tag{11}$$

And the instantaneous doppler frequency ν is given by

$$\nu = f_i - f_o = - f_o \frac{d\tau}{dt} \quad . \tag{12}$$

Estimation of Target Properties

The radar measurements of echo strength, range, and doppler can be used to estimate properties of extended objects. Suppose, for example, that such an object contained several distinct scatterers, then the angular extent of this object can be estimated by analysis of the doppler shifts in the echo that correspond to each scatterer. This can be seen by differentiation of Equation (8) with respect to angle,

$$\delta\nu \cong 2v/\lambda \cos\theta \, \delta\theta \quad ; \tag{13}$$

and, therefore,

$$\delta\theta \cong \frac{\lambda}{2v} \frac{\delta\nu}{\cos\theta} \quad . \tag{14}$$

Thus, by measuring the extent of the doppler shift $\delta\nu$, due to the radar motion relative to the object, the angular extent $\delta\theta$ of the object can be estimated.

Likewise, the extent of an object in range can be estimated by radars with sufficient range resolution. If, for example, the echo from the leading edge of an object can be resolved in time from the echo of its trailing edge, then by Equation (7) the difference between the corresponding ranges is an estimate of the object's range extent.

In addition, the physical size of an object is often related to the power of its echo. For example, one would expect that, in general, the

total received power from a large building would be greater than that received from an automobile. This subject will be discussed in more detail in Section 3.0.

1.4 Radars as Linear Systems

To avoid discussing many of the details on the mechanization of radars, especially the more sophisticated systems such as synthetic aperture radar (SAR), it is desirable to describe a radar system more abstractly as a linear input/output device. An efficient and useful way to do this is to consider a radar system as a linear system.

System Response Function

For any physically realizable linear system, it can be shown that for any input I(t) to the system, the output H(t') is given by

$$H(t') = \int_{-\infty}^{\infty} F(t)I(t-t')dt \quad , \tag{15}$$

where F(t) is the system response function. This relationship is shown diagrammatically in Figure 4.

The linear system response function can be fully described by its response to the unit impulse. The unit impulse is defined as a function $\delta(t)$ whose value is zero everywhere in time, except in an arbitrarily small interval, where its value becomes infinite, such that

$$\int_{-\infty}^{\infty} \delta(t)dt = 1 \quad . \tag{16}$$

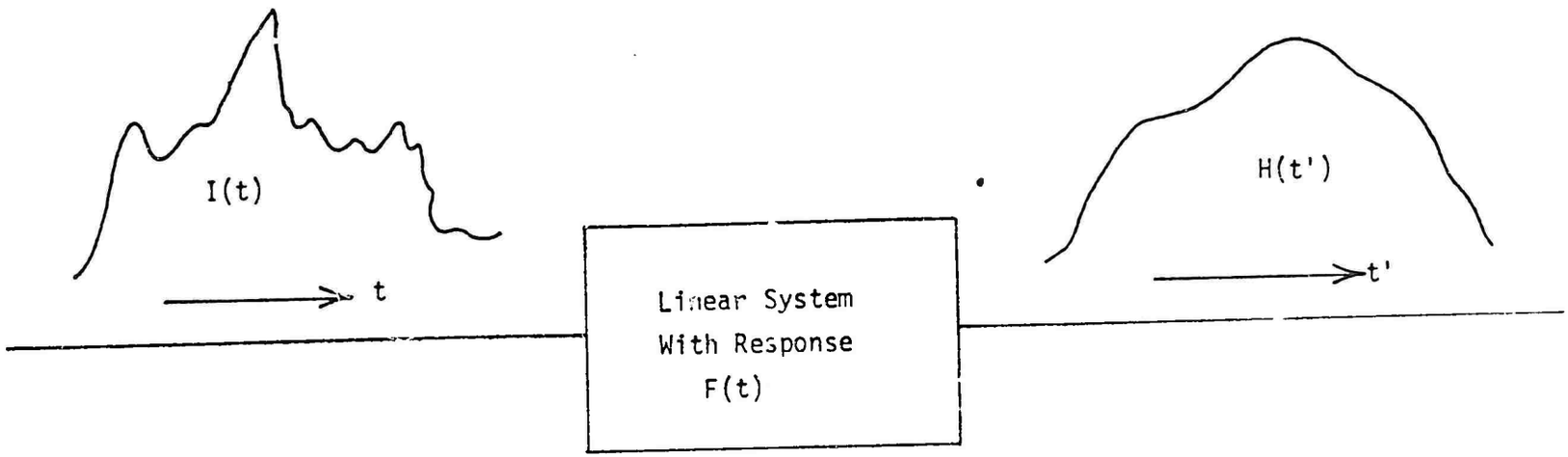

Figure 4. Input/Output Relationships of a Linear System

(Although true unit impulses cannot be generated exactly in practice, close approximations can be realized.)

Since $\delta(t)$ has the property that the convolution of itself with any given function yields that same function back, in particular,

$$F(t') = \int_{-\infty}^{\infty} F(t)\delta(t-t')dt \quad . \tag{17}$$

This relationship is shown diagrammatically in Figure 5.

Radar Impulse Functions

Radars, being linear systems, can be described in terms of their response functions, often termed impulse response functions. As suggested pictorially in Figures 4 and 5, the impulse response functions of radars usually perform a smoothing operation on the input. Analogous to the radar beam patterns associated with antennas, the half-power width of the impulse response function is a measure of the radar system resolution. This may be measured in time delay (equivalently, range) or doppler. Figure 6 shows a typical impulse response function for a synthetic aperture radar system. Given a "point scatterer" (i.e., an impulse source) in a radar absorbing background, the output of the radar system would appear ideally much like Figure 6. More realistic outputs would be influenced by the match between the intensity of the radar return and the limited dynamic range of the system (including film storage media). Figure 7 shows examples of how the outputs could vary, assuming that the structure of the impulse response is described by a $\left(\frac{\sin x}{x}\right)^2$ function.

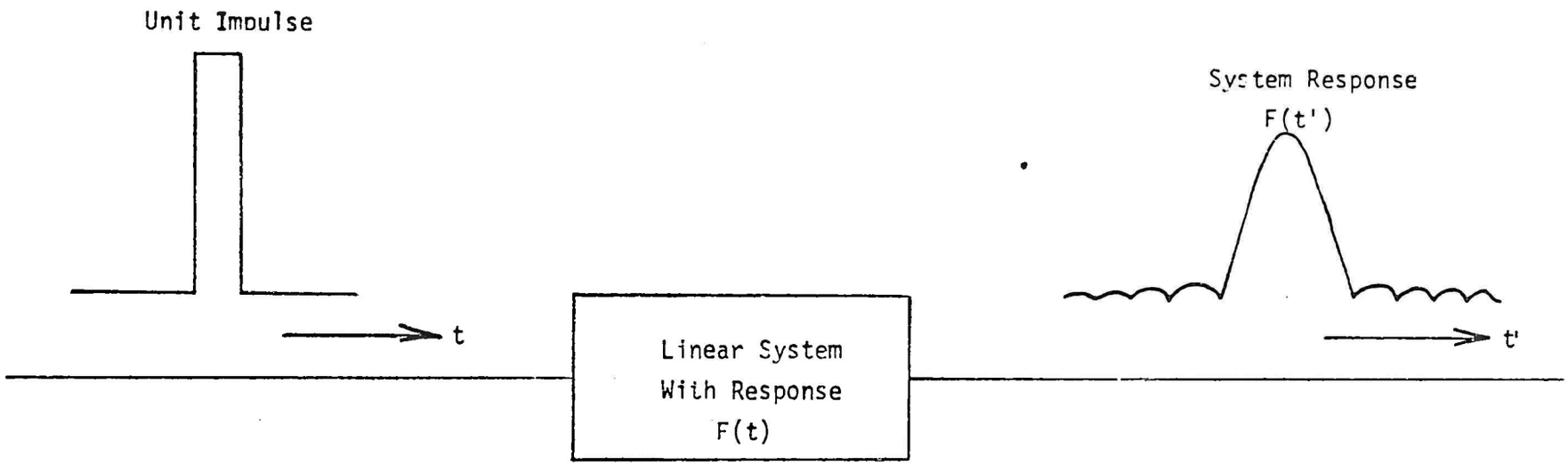

Figure 5. Response of a Linear System to the Unit Impulse

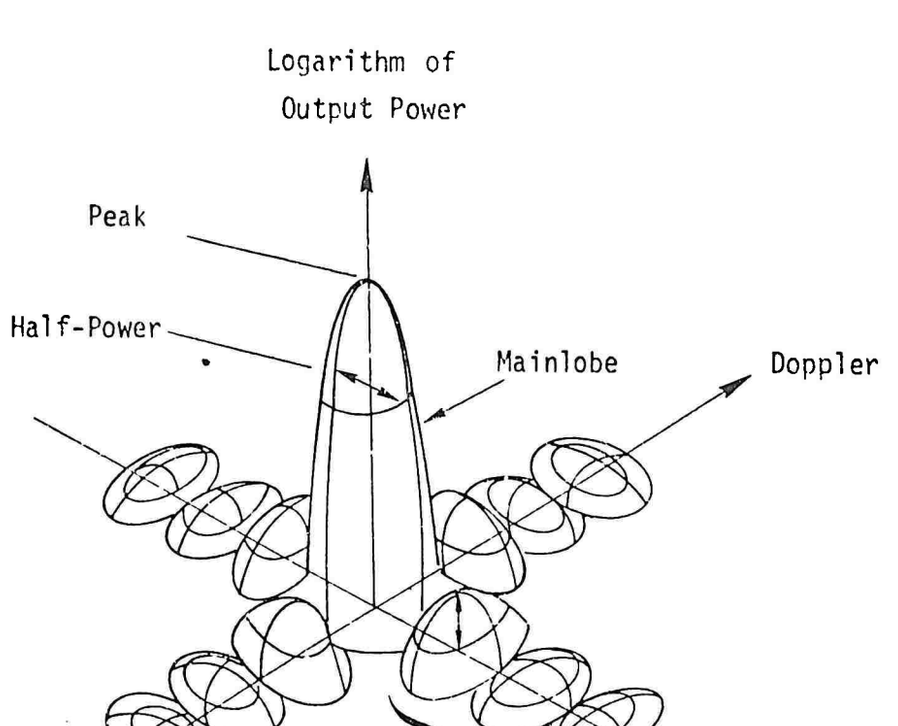

Figure 6. Typical Synthetic Aperture Radar Impulse Response

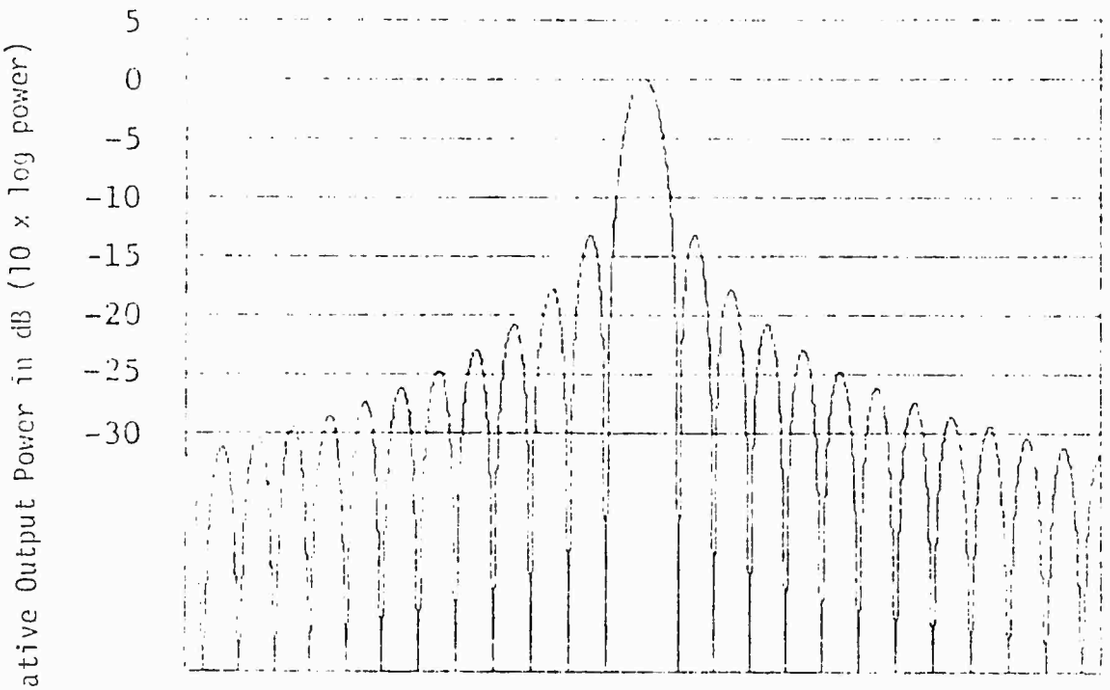

(Sin x)/x Function

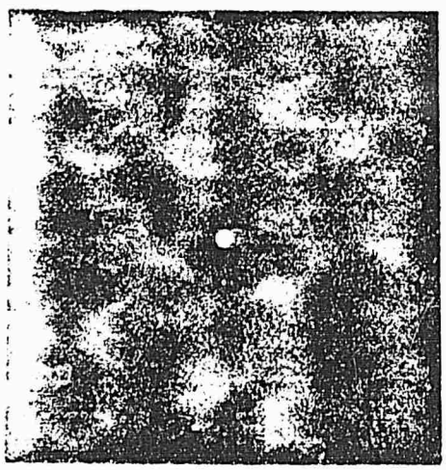

Film Saturation @ 5 dB

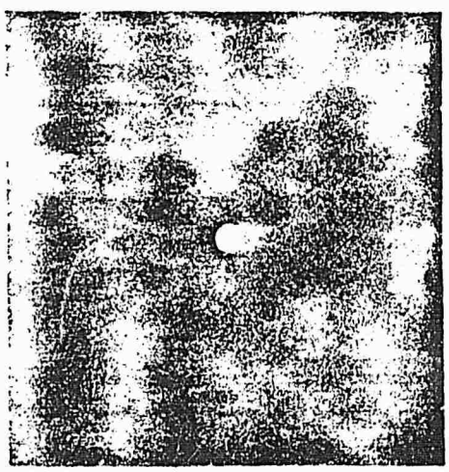

Film Saturation @ 0 dB

Figure 7. Illustration of the Effect of Dynamic Range Limitations on Radar System Output

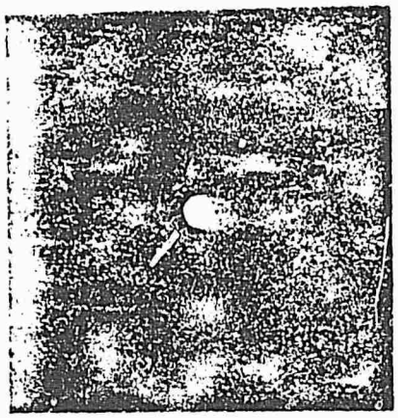

Film Saturation @ -5 dB

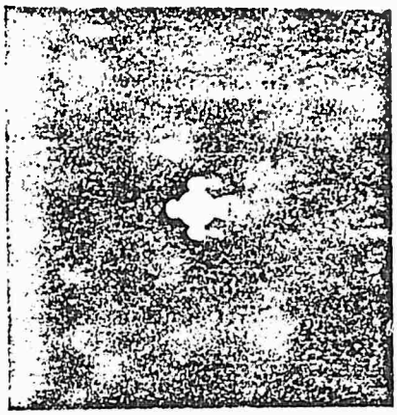

Film Saturation @ -10 dB

Film Saturation @ -15 dB

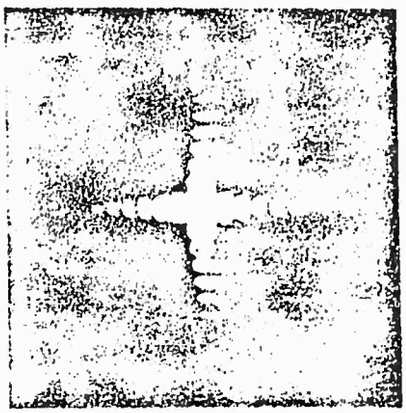

Film Saturation @ -20 dB

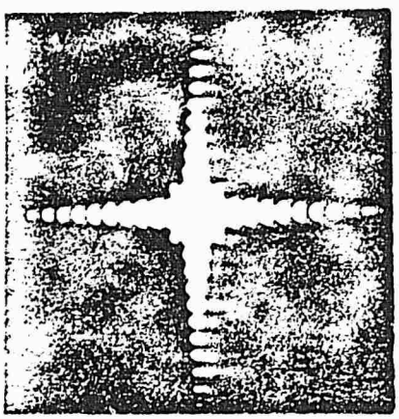

Film Saturation @ -25 dB

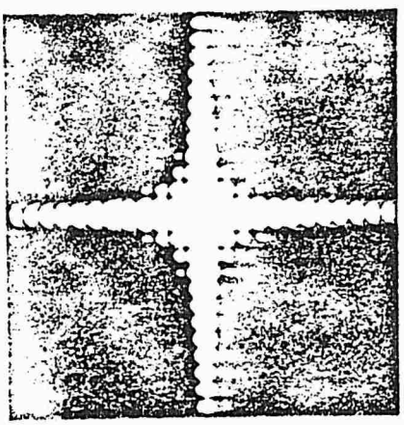

Film Saturation @ -30 dB

Figure 7 (Continued)

1.5 Summary

In this section we have introduced numerous concepts. First of all, a brief introduction was given describing the magnitude and form of the SAR problem facing statisticians and data analysts. Preliminaries were discussed, such as the rationale for the approach taken in this report and the importance of digital/electronic SAR. Next, a survey of radar fundamentals was presented, starting with a discussion of electromagnetic waves and proceeding onto discussions of radar signals and radar antennas. The basic types of radar measurements were then presented. These are range measurement, doppler measurement, and estimation of target properties. Radars as linear systems were then discussed. The radar impulse response function was defined and graphic examples were presented showing typical mainlobe and sidelobe structure, as well as the effect of limited dynamic range on the system output.

2.0 SYNTHETIC APERTURE RADAR

Prior to 1950, the resolution of radars was limited by the ability to resolve differences in time delay in the range dimension and by the narrowness of the antenna beam in the azimuth dimension. However, in the early 1950s, Carly Wiley of the Goodyear Aircraft Corporation concluded that, for a sidelooking radar (see Figure 8), a frequency analysis of the received signals could provide a resolution in the azimuth direction that is much finer than that provided by the physical beamwidth.

Note, for example, Equation (8). When θ is small, $\sin\theta$ can be approximated by $(x-x_0)/R$; and Equation (8) becomes

$$\nu \cong \frac{2V}{\lambda R}(x-x_0) \tag{18}$$

Thus, the doppler shift at any given range R is a linear function of the along-track dimension $(x-x_0)$. Consequently, a frequency analysis of the received signal at any given range provides the $(x-x_0)$ coordinate of each scattering center.

By use of range measurements that involve the use of pulsing and time-delay sorting, as well as the use of doppler or cross-range measurements, a two-dimensional map of radar reflectivity may be generated. This map constitutes the synthetic aperture image.

2.1 Synthetic Aperture Radar Operation

In a radar employing a linear array antenna, the resolution in azimuth is obtained from the antenna beamwidth. In principle, there is no reason why the array elements must co-exist in time provided: (1) the array element positions are known, (2) the transmitted signals are coherent

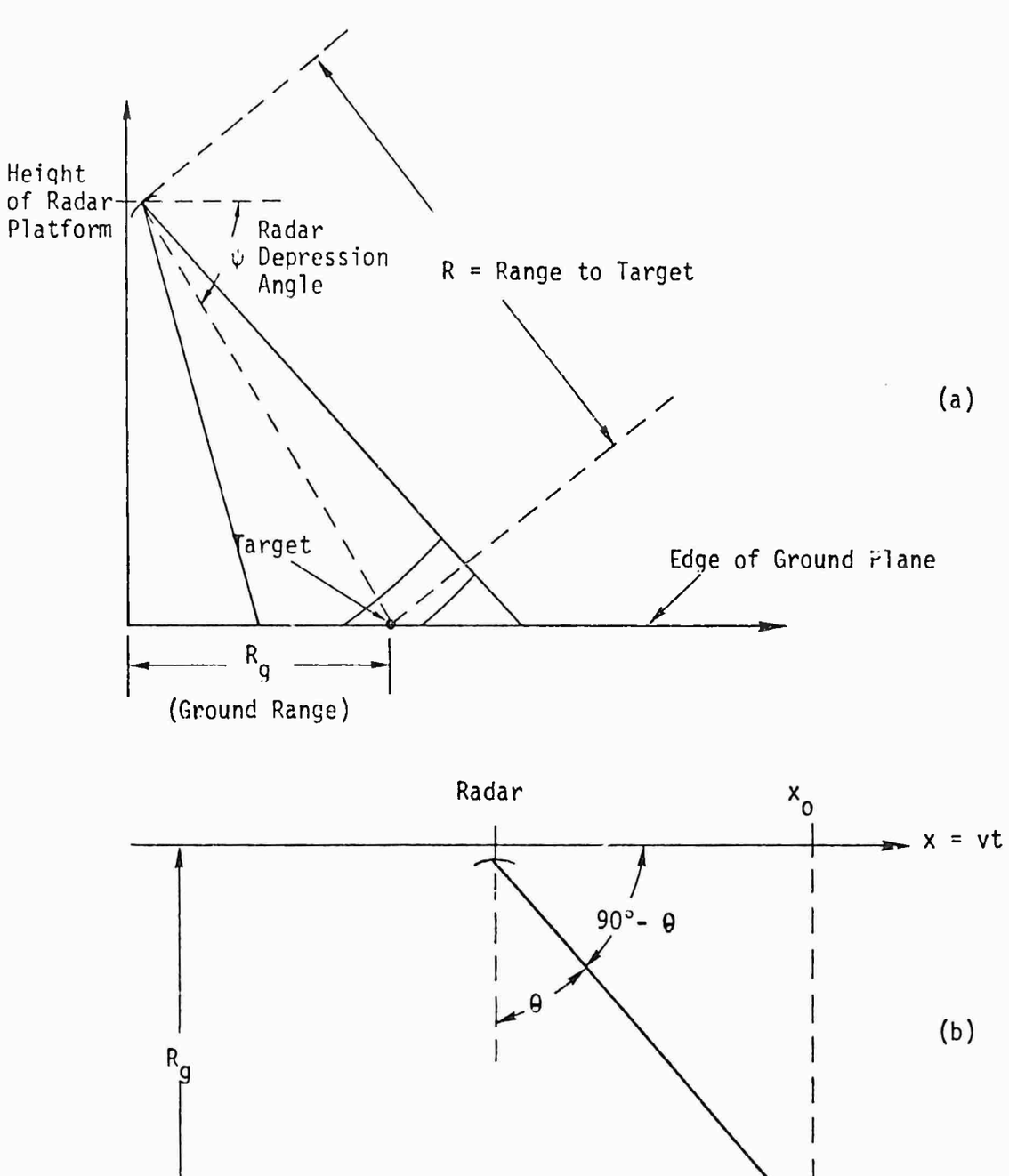

Figure 8. Geometry of Sidelooking Radar:
(a) Vertical Geometry
(b) Geometry in Ground Plane

(i.e., they do not experience phase jitter or phase drift), and (3) the received signals at the elements are coherently stored (i.e., phase information is preserved) and coherently processed with knowledge of element positions as a function of time. Thus, if a coherent radar system were to employ a real antenna (e.g., a small parabolic dish) that successively assumed the positions of the elements of a long linear array antenna, the system would be forming a synthetic array (or synthetic aperture), provided the returns from these successive positions are coherently stored and integrated. The resulting azimuth resolution is essentially that from a long linear array whose length is equivalent to the flight path distance over which the processor coherently stores and integrates the returns.

The three-dimensional configuration is depicted in Figure 9. The radar moves with constant velocity along a straight horizontal path. Through successive transmissions it illuminates a ground swath that lies parallel to the flight path. The radar is pointed broadside to the velocity vector. As the radar moves along its path, it transmits pulses at regular intervals and stores the returns, preserving phase, thus forming a phase history of the received echoes. When all the returns from a given range interval have been accumulated, they are coherently summed to form a narrow beam that is focused on the range interval of interest.

2.2 Resolution

Let D be the dimension of the real antenna, measured in the direction of the flight path; and let L be the length of the synthetic aperture. Since, as shown in Equation (6), the half-power beamwidth β can be expressed as λ/L, the lateral subtense of the synthetic beam at range R can be approximated

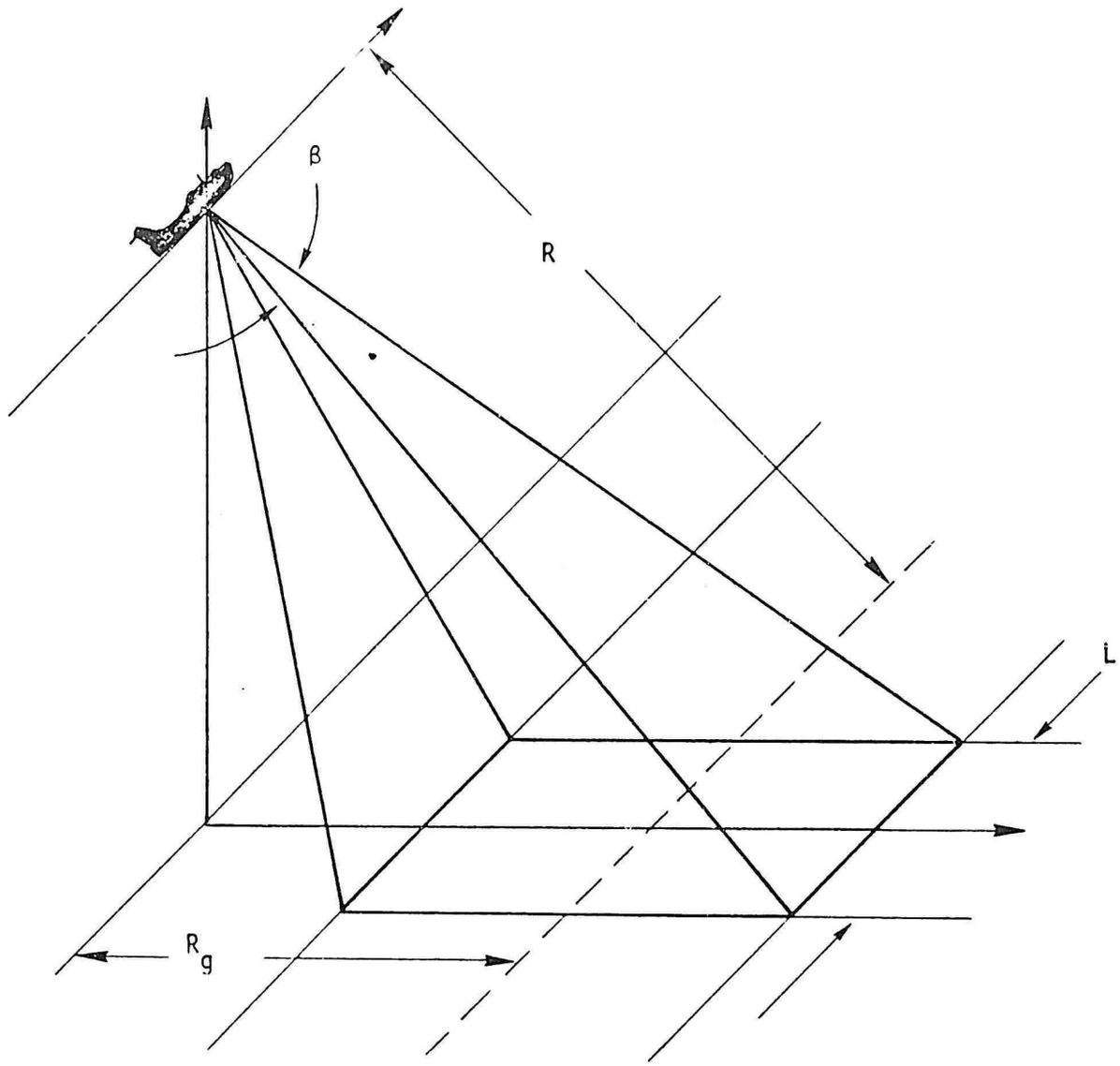

Figure 9. Three-Dimensional Configuration in Synthetic Aperture Radar Operation

by λ/L R. Actually, the usable synthetic aperture length L_u is a function of R also. For example, given a point in the ground swath at range R, it will be well illuminated by the real antenna beam as the radar moves a distance

$$L_u \cong \frac{\lambda}{D} R \quad , \tag{19}$$

where λ/D is the approximate angular beamwidth of the real antenna. Thus, the azimuth or crossrange resolution at range R is given by

$$\Delta x \cong \frac{1}{2} \frac{\lambda}{L_u} R = \frac{D}{2} \quad . \tag{20}$$

(The factor of 1/2 is used for the synthetic beam because it is not just a one-way illumination function, but rather it accounts for the phase shifts that occur going to and from the target.)

Equation (20) shows that the crossrange resolution Δx is a function only of the real antenna dimension. It is very significant that the crossrange resolution Δx is independent of range and wavelength. This is a unique property of synthetic aperture radars.

In addition to resolution in the direction of flight, the radar obtains slant-range resolution through the use of pulsing and time-delay sorting. If the pulse is very short, say of duration $\Delta\tau$, then the returns from targets at sufficiently different ranges will be separated in time by at least one

pulse duration. Differentiation of Equation (7) shows that the required separation in range is given by

$$\Delta R \geq \frac{c\Delta\tau}{2} \tag{21}$$

Using this as a measure of slant-range resolution ΔR, then the corresponding resolution in the "ground plane" (i.e., ground-range resolution) is given by

$$\Delta G = \frac{c\Delta\tau}{2} \sec \psi \quad , \tag{22}$$

where ψ is the depression angle of the line-of-sight to the target.

2.3 Raw Data Recordings

Typically the signals received from a target are adjusted in doppler frequency and normalized in intensity and then recorded on film. Figure 10 is a schematic of the technique whereby signals are displayed on a cathode ray tube (a television) and recorded on film. From Equation (18) we saw that, for any given range, the doppler shift is a linear function of the along-track displacement from x_o. Since instantaneous frequency f_i is given by the sum of the carrier frequency and the doppler shift, the general form of f_i is given by

$$f_i = f_o + \frac{2V}{\lambda R}(x - x_o) \tag{23}$$

Thus, the biased amplitude of the received signal S'_R, given by

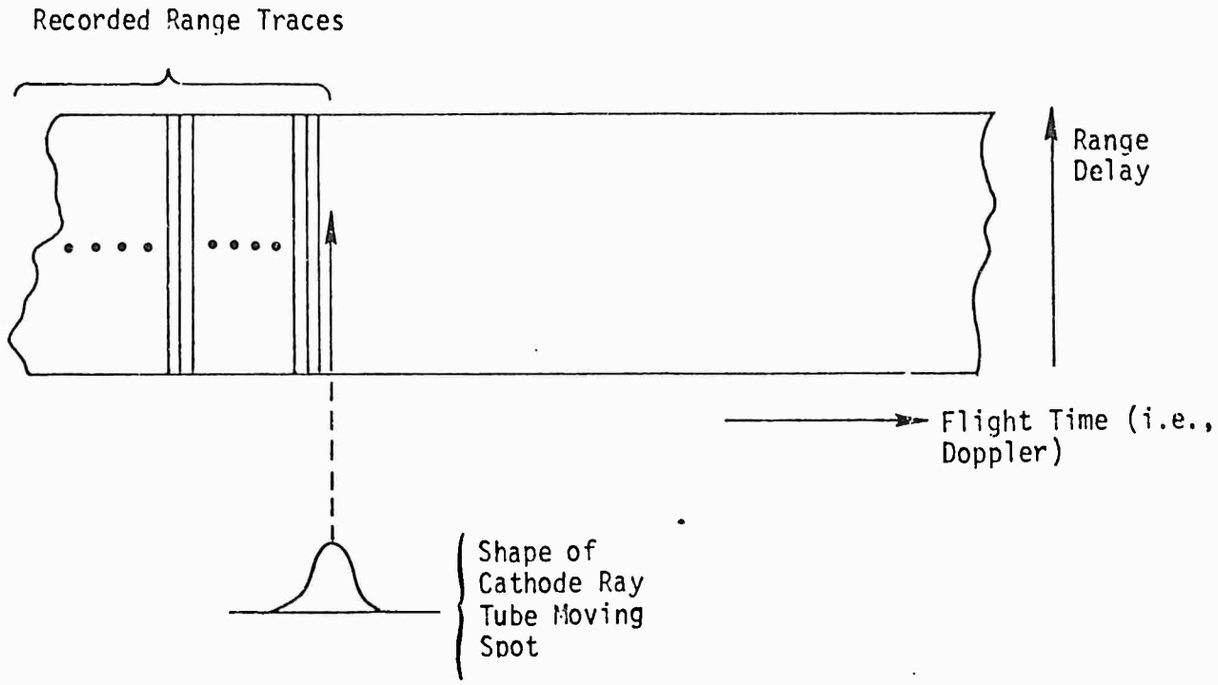

Figure 10. Recording Signals on Film
(From Reference 2)

$$S'_R = A_R \cos (2 f_i t) + B \quad , \tag{24}$$

where B is a positive bias added to the cathode ray tube (CRT) signal to avoid negative values. S'_R will vary as shown in Figure 11. In subsequent processing steps, this bias will be removed. (Therefore, equations in the following discussions of this paper will omit this term.) The side-by-side recording of successive received pulses as the radar moves along its path yield a one-dimensional hologram of the target in the azimuth direction.

Although the natural motion phenomena cause this modulation of the signal in azimuth, a similar modulation can be, and usually is, employed within each pulse by changing the instantaneous frequency linearly with time. This is called a linear FM signal. (FM signals are commonly employed by a large class of radars called pulse compression radars. Rather than digressing to the subject of pulse compression technology, we shall simply assume that signal modulation and pulse compression can be achieved.) The result of employing linear FM is to create a two-dimensional hologram of the target. Figure 12 shows a plot of the signal recordings for a stationary point target due to linear FM and the radar's linear motion. Any cut through the depicted surface in the horizontal direction is the linear FM modulation of a pulse. (There are several advantages to using frequency modulated signals, especially with regard to gaining high resolution while maintaining target detectability and reasonable power requirements. Other types of modulation may also be used, however.

If the amplitude variations are properly recorded on film (including the scaling of displacements to optical wavelengths), an optical processor can integrate the signals in both range and azimuth in one operation to obtain a target image. (The optical processing can also be performed sequentially in

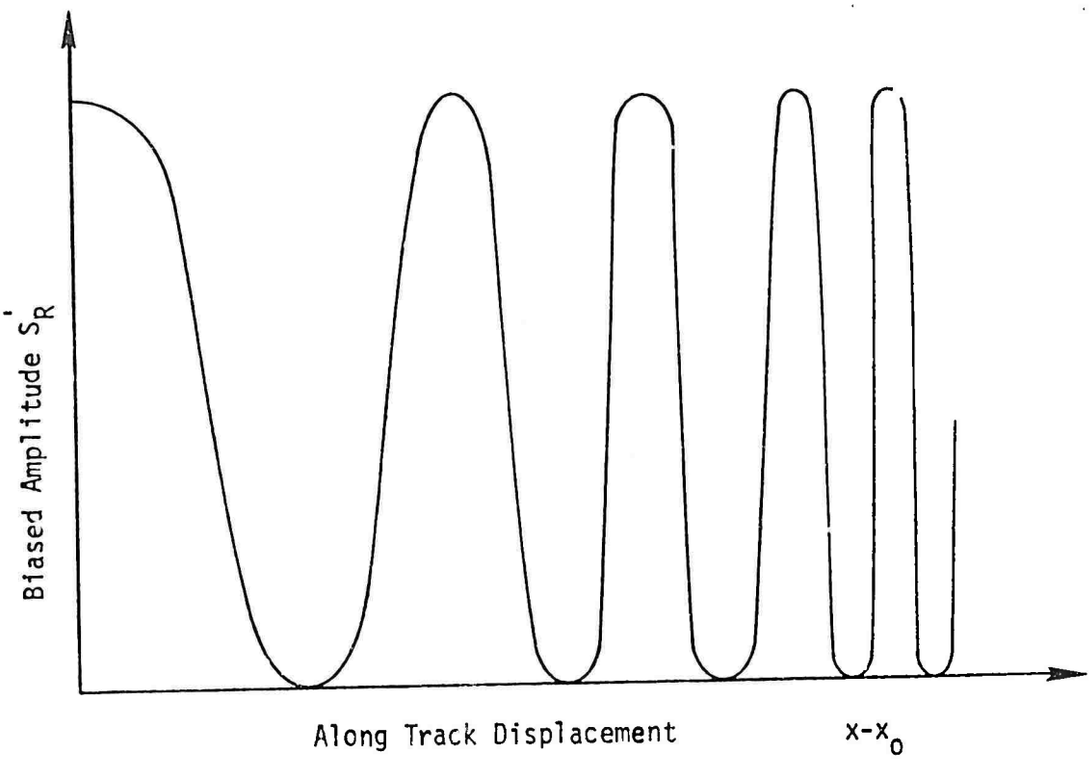

Figure 11. Recorded Amplitude Variations for the Received Signal from a Target

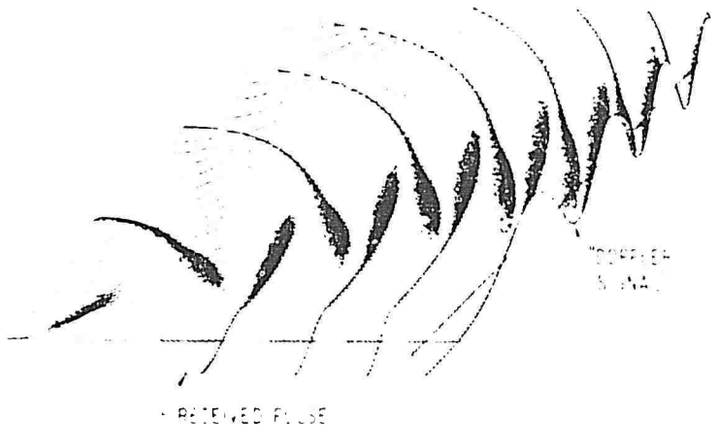

Figure 12. Signal Recordings for a Stationary Point Target for Linear Radar Motion and a Linear FM Waveform

(From Reference 3.)

range and azimuth. In the range dimension, this process would be called optical pulse compression.)

2.4 Optical Processing

Figure 13 shows an example of the signal recordings on film transparency for a point scatterer, from x_o to $x_o + L_u/2$. This segment of the signal recording forms a portion of a Fresnel zone plate. (A Fresnel zone plate acts as a lens which may be illuminated with a coherent light source, such as a laser, to form a coherent two-dimensional image, as in holography.)

In principle, the way in which a Fresnel zone plate forms an image is as follows: As viewed from the side, the Fresnel zone plate appears as in Figure 14, where the path lengths R(x) from adjacent opaque and transparent rings to the image focal point differ by $\lambda/2$, (λ is now the optical wavelength and distances x and R are scaled by the ratio of the optical wavelength to the radar wavelength). Let R_o be the perpendicular distance from the zone plate to the focal point. Due to the differences in path length to the image point, it is clear that if the black rings were transparent, the coherent illumination passing through adjacent rings would cancel at the focal point. However, since we may consider the black rings as opaque, only the light passing through the transparent rings is summed at the focal point. But this light will reinforce by adding in phase since the phase of the coherent illumination coming from alternate rings is spaced one wavelength apart.

When considering the composite Fresnel pattern of multiple targets and their resultant images, the linearity of the total system allows for separate images to be formed. From the discussion above, we have seen that when a reflecting object or scatterer is located at a scaled range R_o and at a scaled crossrange on the film of x_o, then the coherent summation of the light passing through the

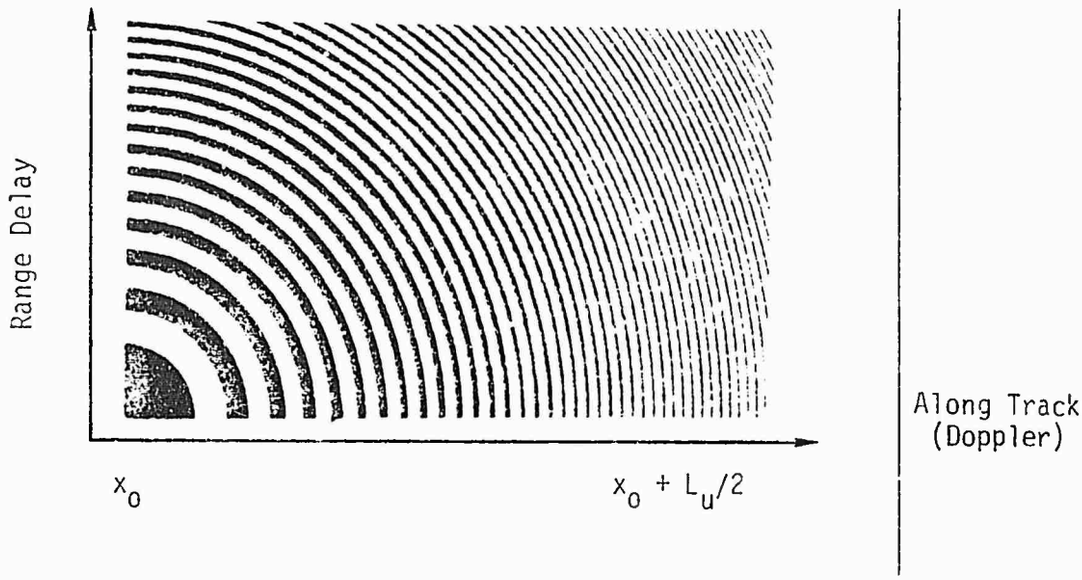

Figure 13. Example of Signal Recordings on Film Transparency for a Point Scatterer Located at x_o
(From Reference 3.)

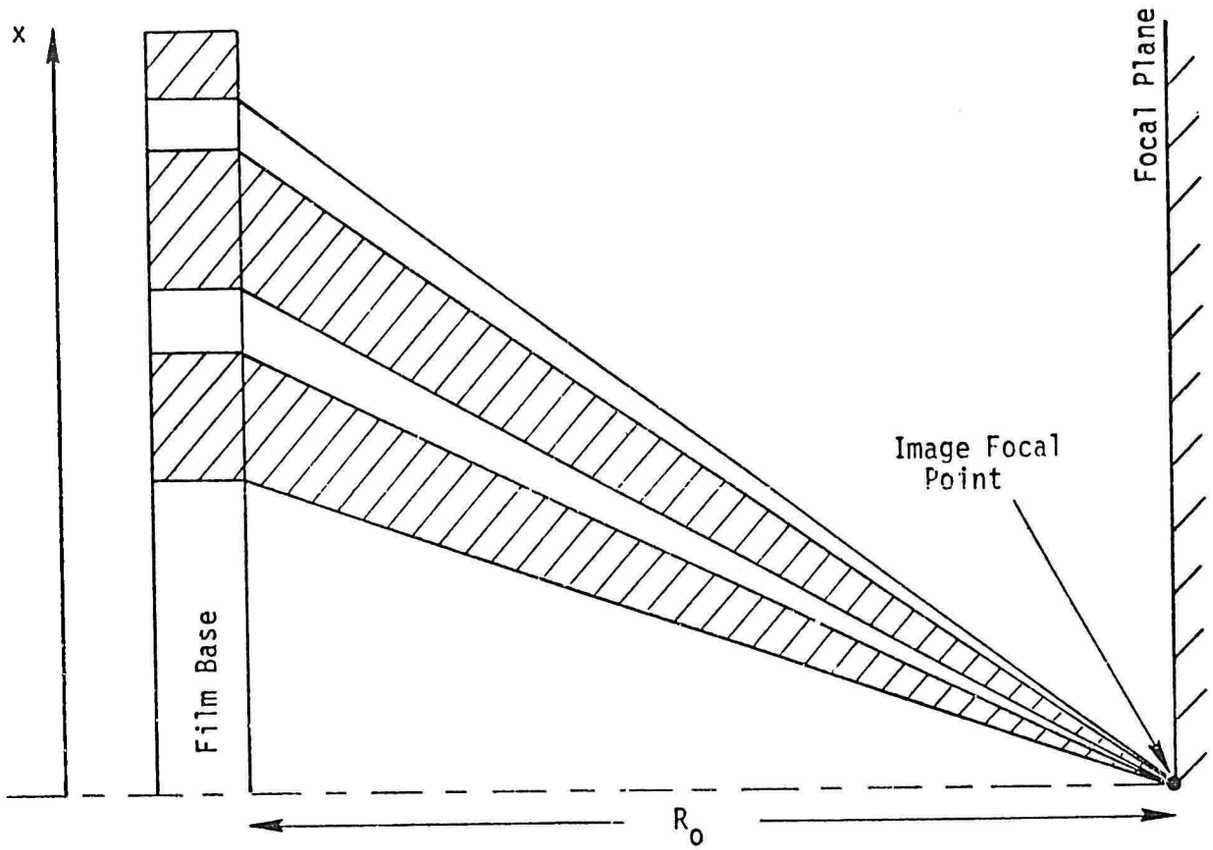

Figure 14. Side View of Fresnel Zone Plate

aperture extending from x_o to $x_o + L_u/2$ will reinforce. Although secondary reinforcement may take place at crossrange locations other than x_o, the intensity of these secondary reinforcements will be much lower than the primary reinforcement at x_o. Let us define the signal focused at x_o for a single scatterer by

$$S_f(x_o) = \int_{x_o}^{x_o+\frac{L_u}{2}} A(x) \cos(2\pi\frac{R}{\lambda})dx \quad , \tag{25}$$

where A(x) is the amplitude of the illumination passing through the film at x. The range to the focal point is given by

$$R = R_o + \Delta R \quad , \tag{26}$$

For small displacements $x - x_o$, this can be approximated by

$$R \cong R_o + \frac{(x-x_o)^2}{2R_o} \quad , \tag{27}$$

since

$$(x - x_o)^2 = (R_o + \Delta R)^2 - R_o^2 \tag{28}$$

and

$$(x - x_o)^2 \cong 2R_o \Delta R \quad . \tag{29}$$

Therefore

$$S_f(x_o) = \int_{x_o}^{x_o+\frac{L_u}{2}} A(x) \cos\left\{\frac{2\pi}{\lambda}\left[R_o + \frac{(x-x_o)^2}{2R_o}\right]\right\}dx \quad . \tag{30}$$

Since each resolution interval $\Delta R >> \lambda$, we may assume, without loss in generality, that R_o is an integral number of wavelengths. Thus, whenever $\Delta R = n\lambda$, the integrand reduces to $A(x)$. And the total signal at the focal point is approximated by

$$S_f(x_o) \cong \sum_{i=1}^{m} A_i \, \Delta x_i \quad , \tag{31}$$

where Δx is the width of the i^{th} transparent Fresnel ring, A_i is the transmitted intensity, and m is the number of Fresnel rings.

Going back to the actual radar geometry for a moment, suppose that there are now several random scatterers at range R_o, but at different azimuths, whose stored signal records have added vectorially (i.e., in phase and amplitude) to produce a more complicated composite Fresnel pattern. For example, if the j^{th} scatterer is located at azimuth x_j, with an initial <u>random</u> phase upon reflection of ϕ_j and amplitude $A_j > 0$, the composite signal at x recorded for J scatterers is given by

$$S(x) = \sum_{j=1}^{J} A_j \cos \left[\frac{2\pi}{k\lambda} \frac{k^2(x-x_j)^2}{2R_o} + \phi_j \right] \quad , \tag{32}$$

Upon illumination of the data film, the amplitude of the signal transmitted through the film at x would be equal to the amplitude of S(x), where, for clarity, λ is the optical wavelength of the processor and $k\lambda$ is the radar wavelength. Notice that the scale factor k cancels out of the equation. For a set of Rayleigh random scatterers, the amplitude of the summation in Equation (32) may be approximated by

$$|S(x)| \cong \sqrt{\sum A^2_j} \tag{33}$$

The phase would, of course, be random over 2π radians.

If we now superimpose the return $A(x)$ from the scatterer located at x_o, which was previously discussed, we have the total recorded signal

$$S_T(x) = S(x) + A(x) \tag{34}$$

So the signal focused at x_o is now given by

$$S_f(x_o) = \int_{x_o}^{x_o + \frac{L_u}{2}} \left[S(x) + A(x)\right] \cos\left\{\frac{2\pi}{\lambda}\left[R_o + \frac{(x-x_o)^2}{2R_o}\right]\right\} dx \tag{35}$$

analogous to Equation (30).

But, $S_f(x_o)$ can be decomposed into two parts: the image of the scatterer located at x_o and the superposition of secondary images of a field of random scatterers.

$$S_f(x_o) = \int_{x_o}^{x_o + \frac{L_u}{2}} A(x) \cos\left\{\frac{2\pi}{\lambda}\left[R_o = \frac{(x-x_o)^2}{2R_o}\right]\right\} dx$$

$$+ \int_{x_o}^{x_o + \frac{L_u}{2}} S(x) \cos\left\{\frac{2\pi}{\lambda}\left[R_o + \frac{(x-x_o)^2}{2R_o}\right]\right\} dx \tag{36}$$

The first term is identical to Equation (30), namely, the image of the scatterers located at x_o. The second term is the image resulting from the systematic superposition of the returns from a field of scatterers with random phases (see Equation (32)). In general, the image of the focused scatterer

at x_0 will be much brighter than the superimposed secondary unfocused image of random scatterers.

2.5 Summary

In this section we have shown the fundamental linear relationship between the along-track dimension $x-x_0$ and the doppler shift ν and how this relationship may be used in the generation of two-dimensional (range and doppler) radar reflectivity maps. We have discussed the operation of synthetic aperture radar systems, their geometries, the functional form of their resolution, the storage of raw data (phase histories) on film, the linear FM signal and two-dimensional holograms (fresnel zone plates). A detailed development of optical processing was presented, including equations for correlation (i.e., integration) of the phase histories for single and multiple targets.

3.0 RADAR TARGETS

In order to fully comprehend SAR data, one must understand not only SAR systems, but also radar targets. The definition of the term "target" is mission dependent. For example, the radar image of a body of water may serve as a key navigation aid in one context; and, in another context, it may be only the background for the image of a ship.

3.1 Radar Cross Section

Two important and interrelated properties of radar targets are their scattering efficiency and their directionality. Scattering efficiency, or radar cross section σ, is defined as

$$\sigma = \left[\begin{array}{l}\text{intercepted} \\ \text{area of object}\end{array}\right] \times \frac{\left[\begin{array}{l}\text{power reflected in the} \\ \text{direction of the antenna} \\ \text{per unit solid angle}\end{array}\right]}{\left[\begin{array}{l}\text{incident power in the} \\ \text{direction of the antenna} \\ \text{for isotropic reflection}\end{array}\right]}. \qquad (37)$$

The term "isotropic" means reflected with equal intensity in all directions. Thus the radar cross section σ is proportional to the intercepted area of the object and the power density reflected toward the antenna. The denominator is a normalization factor.

For most radar targets σ is a function of the direction of the incident energy; that is, σ is a function of the location of the radar. The variation of σ with radar direction is a measure of a target's directionality. Targets which exhibit a rather uniform variation of σ in elevation angle ψ and azimuth angle θ are called isotropic scatterers. (See Figure 15.) Targets which exhibit a markedly

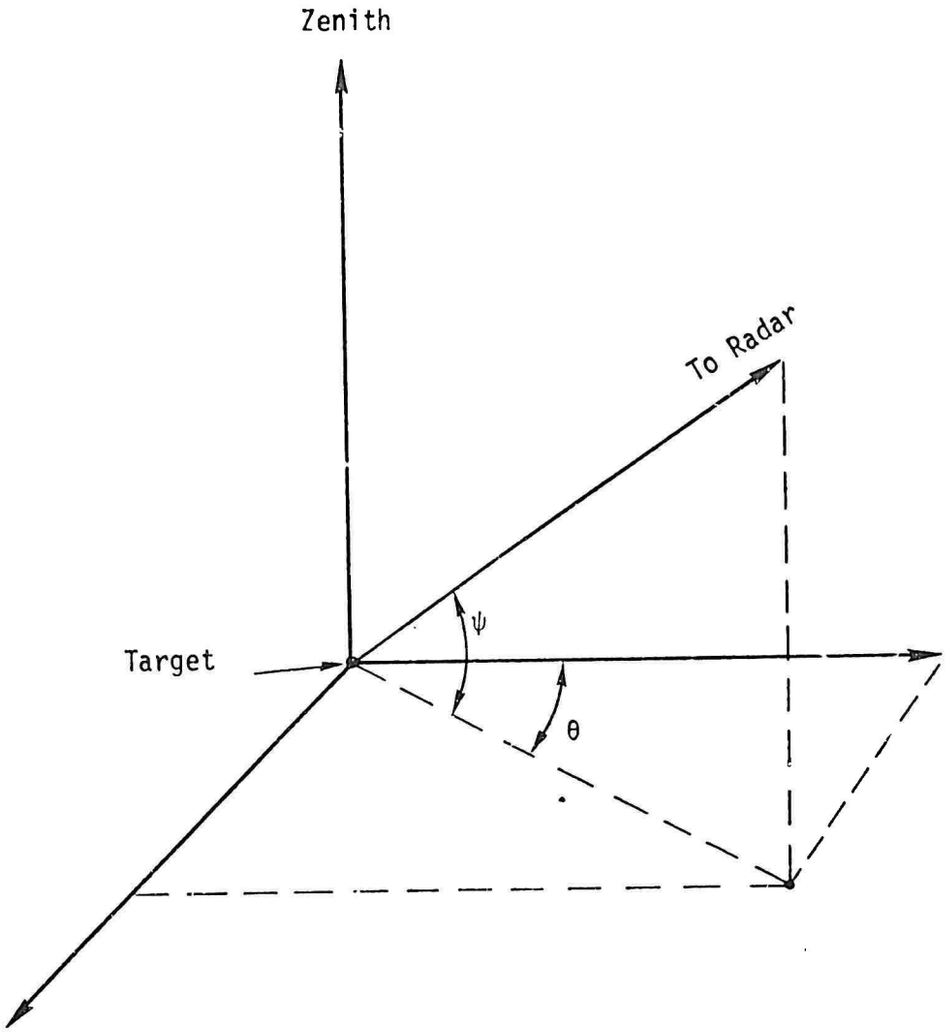

Figure 15. Coordinates of Elevation and Azimuth

enhanced value of σ over a small range of ψ and θ are called directional scatterers. The degree to which they vary between these two extremes is called their directionality.

The magnitude of the radar cross section is a function of the size, shape, conductivity, dielectric constant, surface roughness and orientation of the reflecting object. For scatterers whose dimensions are less than $\lambda/2\pi$, the scattered field is weak and isotropic. The units of radar cross section are ft^2 or m^2. Due to the large dynamic range of radar cross section, it is often expressed in decibels (dB) which are defined as $10 \times \log_{10}\sigma$.

Figures 16 and 17 show the idealized radar cross section as a function of angular displacement for typical scatterers whose dimensions are, at least, several wavelengths long. These scatterers are the flat plate, the cylinder, the trihedral corner reflector, and a pair of point scatterers. Table 1 summarizes their scatter patterns. Note that the major lobe width of the flat plate is λ/L, just as though it were a radar antenna. In fact, many radar targets may be modeled as radar antennas. An important radar target that has a similar scatter pattern, at least in one direction, is the dihedral corner reflector. It is important because it can produce strong radar returns and it occurs often in the form of a vertical man-made surface and the ground plane.

Figure 18 illustrates a coordinate system for a dihedral geometry. In this system let the direction cosines of the radar be (λ,μ,ν), then upon double reflection from the two surfaces shown, the direction of the outgoing signal will appear as though it came from a virtual transmitter with direction cosines of $(-\lambda,\mu,-\nu)$. In the case of rectangular flat

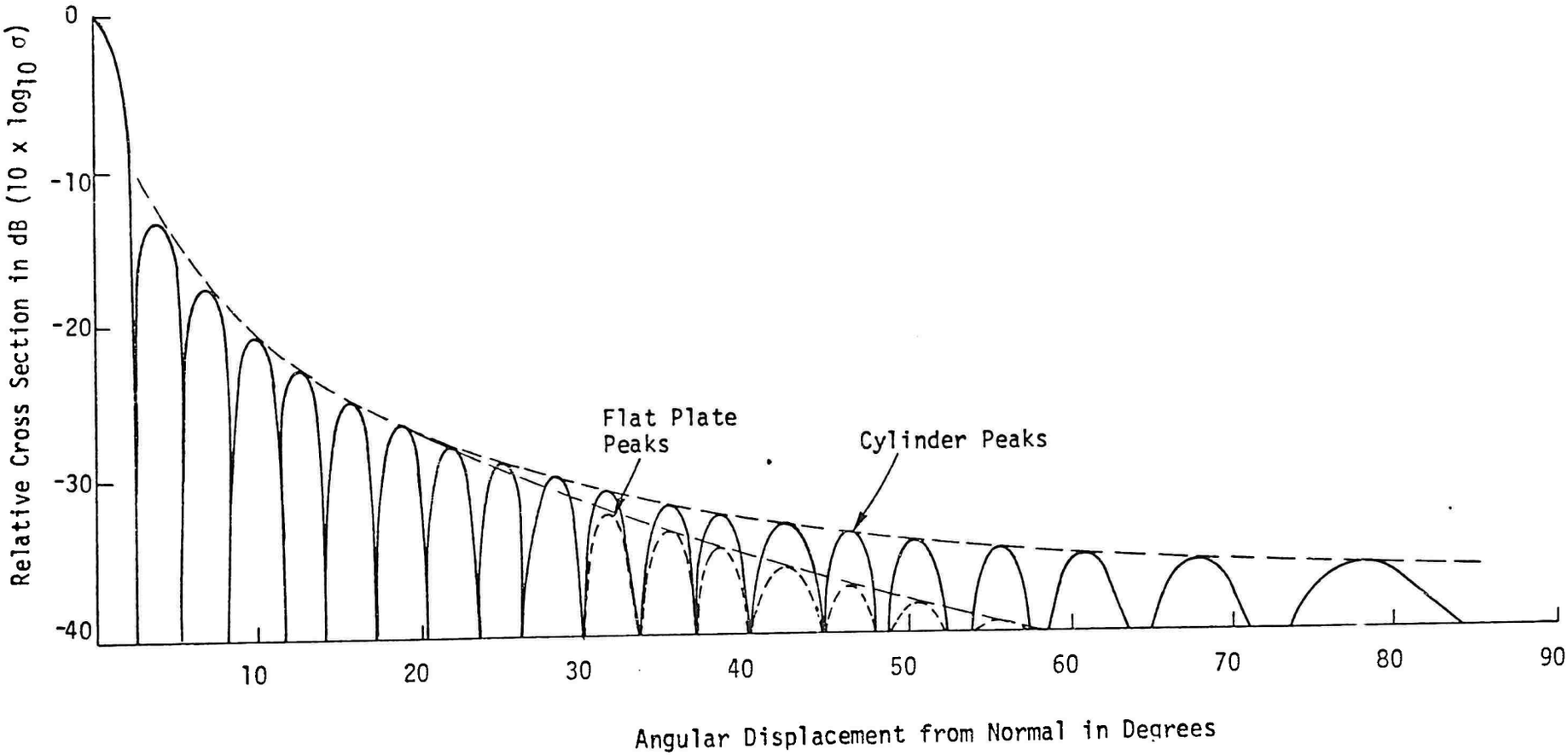

Figure 16. Reflectivity Pattern for a Cylinder and a Flat Plate
(From Reference 4)

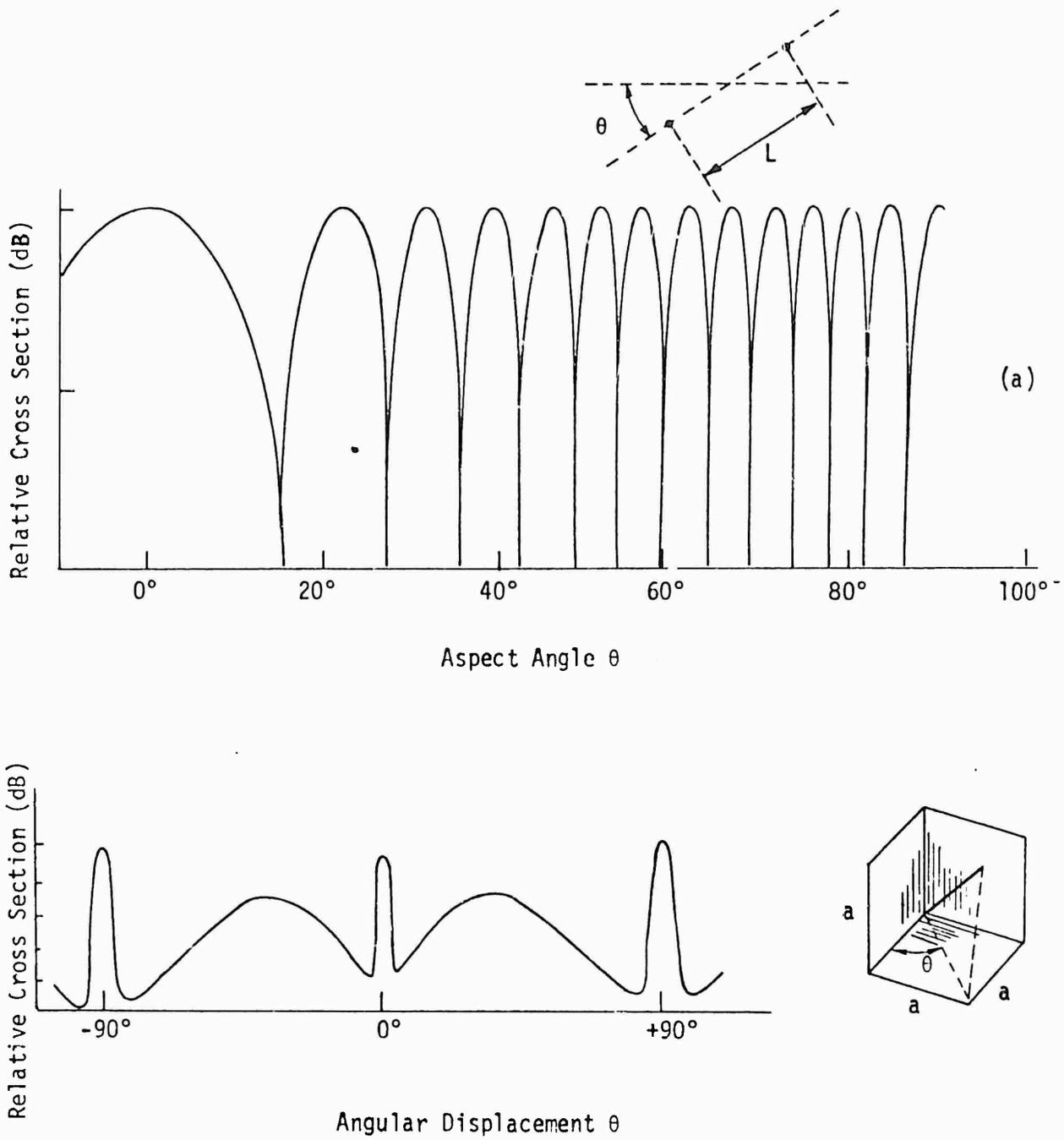

Figure 17. Reflectivity Patterns for:
(a) Dumbbell Reflector
(b) Concave Corner Reflector
(From Reference 4)

Table 1. Radar Reflectivity Characteristics of Simple Bodies (Reference 4)

Object	σ_{max}	σ_{min}	Number of Lobes	Major Lobe Width
Cylinder*	$\frac{2\pi\alpha L^2}{\lambda}$	null	$\frac{8L}{\lambda}$	$\frac{\lambda}{L}$
Flat plate**	$\frac{4\pi A^2}{\lambda^2}$	null	$\frac{8L}{\lambda}$	$\frac{\lambda}{L}$
Square corner reflector	$\frac{12\pi\alpha^4}{\lambda^2}$		4	$\frac{\pi}{4}$

*α is the radius and L the length of the cylinder.

**A is the area of the flat plate and L the length of its side.

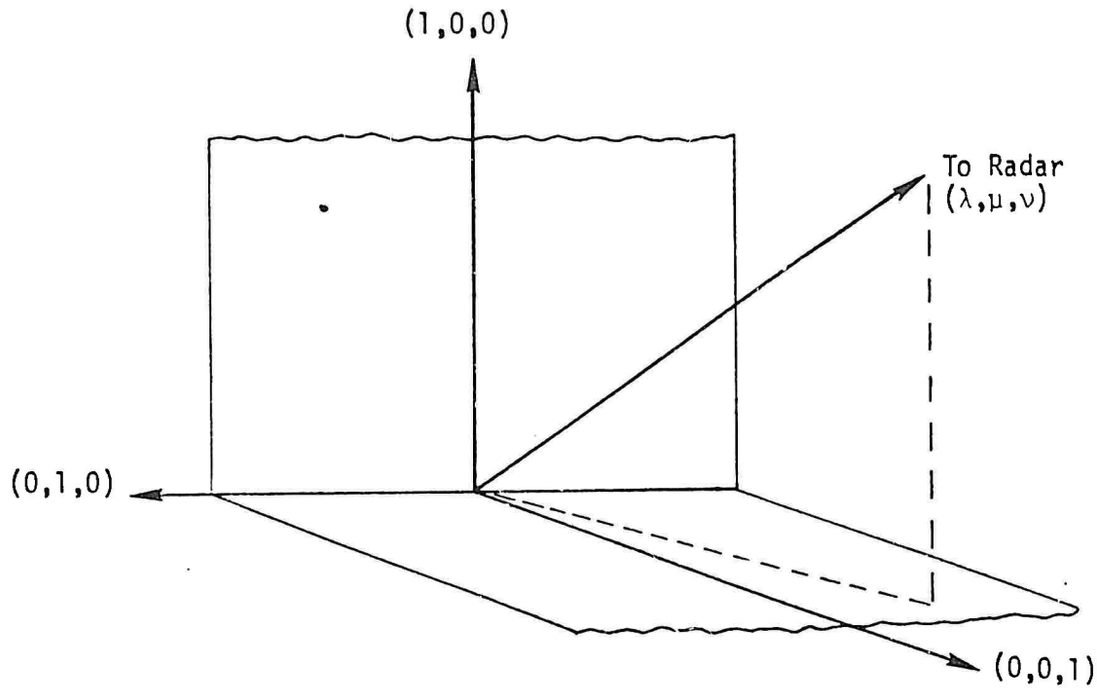

Figure 18. Coordinate System for Multipath Reflections from a Dihedral

plates forming a dihedral, this combination of direction cosines implies that the receiver (located at (λ,μ,ν)) will always be situated on one of the principal axes of the reradiation pattern.

3.2 Terrain and Ocean Background

While the usual emphasis is on man-made targets, the imagery of many man-made targets includes terrain or ocean backgrounds. In addition, the radar return from man-made targets can be greatly influenced by forward scattering off the terrain or ocean surface due to multiple reflections between these surfaces and the target. Furthermore, the radar return from the terrain or ocean surface due to backscattering produces a "clutter" background in radar imagery. For detection of targets in the presence of clutter, one must consider the contrast between their images and the background. Accordingly, consideration must also be given to the terrain and ocean features in any discussion of SAR imagery.

Backscattering

Compared to the peak returns from large flat surfaces and the corner geometries of buildings, the backscattering from terrain and the ocean will be relatively weak. Terrain or ocean surfaces may be modeled as collections of random scatterers with a certain number of discrete scatterers. In general, the return will also tend to be isotropic.

Radar backscattering from the ground is conveniently described in terms of the normalized coefficient σ_0, the radar cross section per unit area illuminated on the ground. Based on a many-scatterer mechanism, σ_0 is the

average of a random process. In many analyses and simulation programs, σ_o has been assumed to be spatially uniform with, at most, a grazing angle dependence. For most applications, however, such an assumption is not realistic and can lead to serious errors.

A quantitative description of the spatially nonhomogeneous scattering model involves a specification of σ_o at each point on the ground. Because of the finite size of a radar resolution cell and the fact that scattering properties generally do not vary over short distances, it is sufficient to specify σ_o at certain points on the ground with values in between determined by some spatial correlation function. However, with little loss in generality, it may be convenient to assume that σ_o is constant within a block of resolution cells but independent from block to block.

The return from a particular resolution cell may be expected to fluctuate. This is primarily due to random phasor addition of several scattering centers in that cell. If no single scattering center predominates, then the resulting amplitude cell fluctuation statistics versus viewing angle approach a Rayleigh density. (See Appendix A.)

The Rayleigh approximation breaks down either when a single scattering center dominates or when there are only a few scatterers in each cell. In this case, any math model must include such scatterers. In most situations a scatterer of this type is isotropic. In some cases, however, the directionality of the scatterer may be important.

Forward Scattering

The forward scattering usually must be defined for the terrain or water surrounding man-made targets. This requirement is due to the ground surface acting as part of a multiple reflecting geometry. The forward scattering coefficient ρ of the sea, for example, may be modeled as

$$\rho = \exp\left[-2\left(\frac{2\pi H \sin \psi}{\lambda}\right)^2\right] \quad , \tag{38}$$

where H = 0.35 × (crest-to-trough waveheight) and ψ is the elevation angle to the radar. (Reference 1.)

(The forward scattering by the sea can affect the observed radar cross section of ships by more than an order of magnitude.)

3.3 Fluctuation Statistics

As can be seen from Figure 16 a slight change in angle can cause a large change in the idealized radar cross section or received power. Since actual radar targets are almost universally non-ideal, their scattering patterns are irregular and unpredictable; and, thus, the magnitude of their returns at any point in time is a statistical phenomenon. If, for example, there are many isotropic scattering elements of comparable size and with phase relationships that are random, as previously mentioned, it can be shown that the probability distribution of cross section is an exponential function (or Rayleigh amplitude distribution, where amplitude = $\sqrt{\text{power}}$). Figure 19

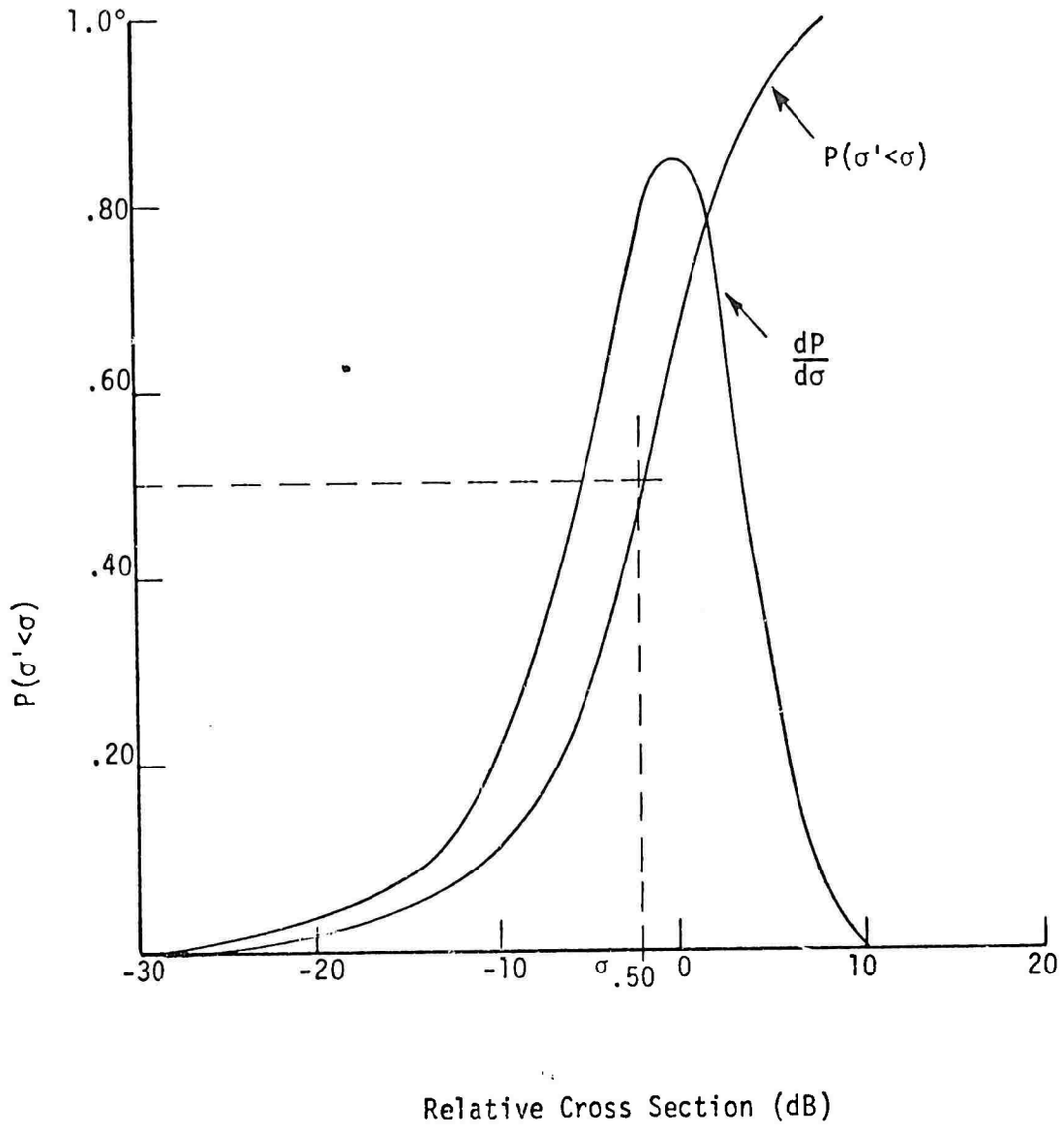

Figure 19. Illustration of Exponential Distribution and Corresponding Density

gives a sample plot of the density and distribution of radar cross section for such a target. If, on the other hand, there is one large dominant scatterer and several other smaller scatterers (for example, when the radar line-of-sight is pointed almost normal to a smooth flat surface), then the statistics of the received power or radar cross section may be adequately modeled with a log-normal distribution. Intermediate situations in which there are, for example, a few dominant scatterers have also been modeled. However, these models have not been used often in radar signal analyses.

The resolution of the radar can also affect the fluctuation statistics that are observed. For example, consider the first case where the "target" was composed of many comparable isotropic scattering elements. If the resolution of the radar is sufficient to isolate each scattering element, then each resolved scatterer would appear to have a constant radar cross section and the image of the target would appear invariant with changes in aspect angle.

If the resolution of the radar were sufficient to only isolate pairs of scatterers, then the statistics of the dumbell pattern, as shown in Figure 17a., would govern the pulse-to-pulse fluctuation statistics of each resolution cell. If the lobe width prescribed by the separation of scatterers were very wide compared with the angular excursion of the radar, then it is likely that all the received pulses would be highly correlated. So, if the returns from a given pair of scatterers were reinforcing, then a strong return would be observed for that cell; if, on the other hand, the returns were cancelling, then a very weak return, if any, would be observed for

that cell. This phenomenon is termed "coherent breakup" or scintillation of the image. It makes for difficult image interpretation by breaking up the image into discrete blobs and increasing the variance of images from one pass to the next.

To reduce this effect requires that, somehow, the number of independent samples from pulse-to-pulse be increased such that, by integration, an estimate of the ensemble average is obtained. (To increase the number of independent samples is costly, since it requires more hardware, more power, less coverage, etc.) This may be accomplished, in some cases, through the proper use of frequency agility. In brief, this technique consists of changing the carrier frequency, and thus λ, by a sufficient amount to ensure independence of radar returns. If we let S in this case represent the amplitude of the radar return as a function of carrier frequency, keeping the radar-target encounter geometry fixed, then the autocorrelation function of S can be used to infer the required change in frequency Δf to ensure independence. The lag of the autocorrelation function required for independence is approximately equal to the angular excursion $\Delta\theta$ or the frequency hop Δf that is required to change the phase of the return signal by 90°. Thus, if by some means this amount of phase change is effected between two return signals, they will be independent.

Consider the return from two dominant scatterers that are spaced ΔR apart in range. One can obtain two independent returns from these two scatterers by changing the carrier frequency sufficiently to change the phase ϕ of the return by 90°. In the far field, the relative phase between these two scatterers is given by

$$\phi = 2\pi\left(\frac{2\Delta R}{\lambda}\right) \tag{39}$$

In terms of frequency

$$\phi = 4\pi\Delta Rf/c \quad , \tag{40}$$

where c is the speed of light.

Thus,

$$d\phi = \frac{4\pi\Delta R}{c}\, df \quad . \tag{41}$$

A change in phase of $\pi/2$ radians implies a change in frequency

$$\Delta f = \frac{c}{8\Delta R} \quad . \tag{42}$$

If, for example, ΔR = 25 ft, then Δf would equal about 5×10^6 Hertz (or 5 MHz).

The size of the resolution cell can influence the effectiveness of frequency hopping. Suppose, as may very well be the case, that at the ends of a target there are relatively few strong scatterers and that these scatterers have fairly short extents, say, for example, 5 feet. If the resolution cell is too small, it may include only one scatterer, or possibly two, such that the total extent in range of strong scattering is only 5 or 10 feet. In this case, Equation (42) predicts that for a separation in range of 10 feet, the required change in frequency to obtain

independent samples would be 12.5 mHz. Thus, with a limited radar frequency band, the number of independent samples per pass would be reduced at a resolution of 10 feet as compared with a larger resolution cell that contained other, more widely separated scatterers on the target.

3.4 Summary

In this section we have discussed, in some detail, the nature of radar targets and backgrounds. First of all we discussed the radar cross section (RCS) of targets and the property of directionality. Plots of idealized RCS for flat plates, cylinders, trihedral corner reflectors, and a pair of point scatterers were presented. The importance of the dihedral corner reflector was also mentioned. The forward scattering and backscattering from terrain and the ocean were discussed in some detail. The Rayleigh density model was introduced; and an equation for the forward scattering off the ocean surface was presented. The effect of radar resolution on the observed fluctuation statistics of radar targets was discussed. The use of change in frequency (frequency agility) to increase the number of independent samples of radar returns was discussed. Equations were presented which determined the required change in frequency to obtain an independent sample of the radar return from two point scatterers.

4.0 IMAGERY CHARACTERISTICS

As previously mentioned, the discussion will be limited to optical processed imagery; however, it may be beneficial to remind the reader at this point, that digital/electronic imagery may differ from optically processed imagery in format and sampling rate.

4.1 Physical Characteristics

SAR imagery has usually been presented in the form of long rolls of continuous film transparencies about 5 to 10 inches in width. This film is usually viewed over a diffuse light table equipped with film spools for ease of handling film. The range of intensities (i.e., the dynamic range) that may be viewed in this way is about 1000 to 1.

Another way in which to present SAR imagery is as the output of an optical processor. In this apparatus, one is viewing the image as it is being formed by the hologram. The dynamic range of this presentation is about a million to one. It also offers the viewer the opportunity of adjusting the focal plane. (This may be essential for viewing a moving target with acceleration in the range direction.)

In reports and other hard copy formats, photographic prints may be made with a resultant loss in dynamic range--down to 100 to 1, or less.

4.2 Ideal Imagery

When nonlinear effects are absent, or have been removed, the image produced is easily described as the output of a linear system. If we assume that the amplitude coefficients $A(= \sqrt{\sigma})$ of scatterers in the ground swath are statistically independent and that their initial phases

upon reflection are random with uniform distribution over 2π radians, then the SAR system output z can be expressed analytically as

$$z(x,y) = \int_Y \int_X A(x',y')\ x(x'-x,y'-y)dxdy \qquad (43)$$

where A(x,y) is the surface of amplitude reflection coefficients in the ground swath, X is the domain of integration in azimuth (or doppler), Y is the domain of integration in range (or delay), and $x(x,y)$ is the impulse response of the whole system: transmitter, receiver, signal processor, signal storage, and optical processor. (Figure 6 shows a schematic of an impulse response function.)

Examples

Figure 20 illustrates the system response in azimuth to a pair of point scatterers. As the impulse response is scanned over a pair of point targets, the average response will be as shown in Figure 20b. If the dip between the two principal responses is deep enough, the radar image will be interpreted to be that for two point targets. The minimum separation between the two point targets which allows them to be resolved on the radar image is a function of the impulse response width (i.e., its half-power width). In some cases, the sidelobe responses could be confused with the mainlobe response of a low-level signal.

Figure 21 illustrates the average condition in the image when low-reflectivity areas are adjacent to high-reflectivity areas. Figure 21a hypothesizes a street surrounded by buildings; Figure 21b shows the average

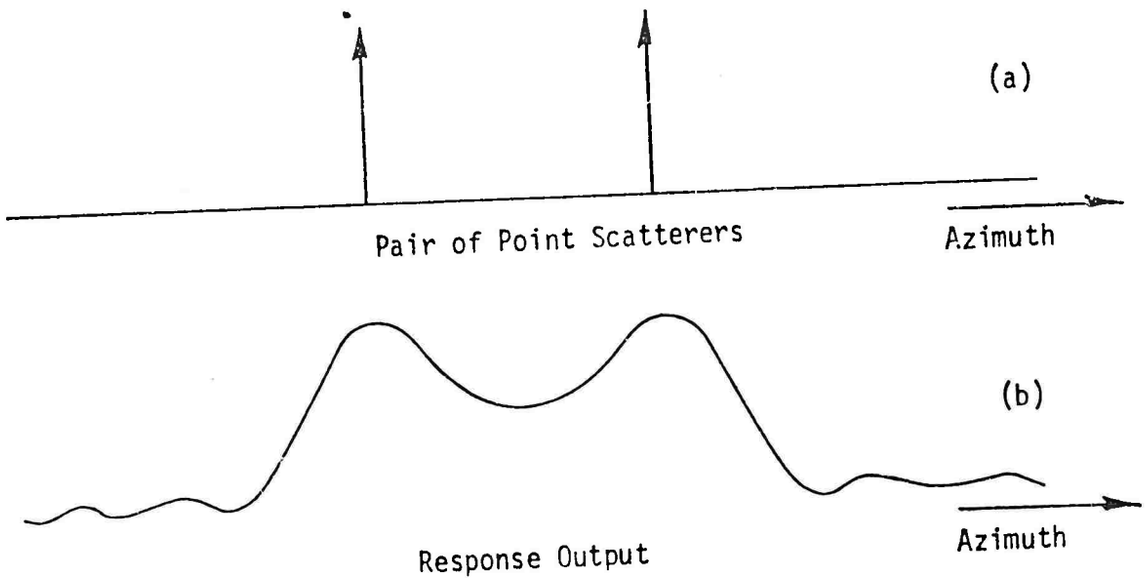

Figure 20. System Response in Azimuth to a Pair of Point Scatterers

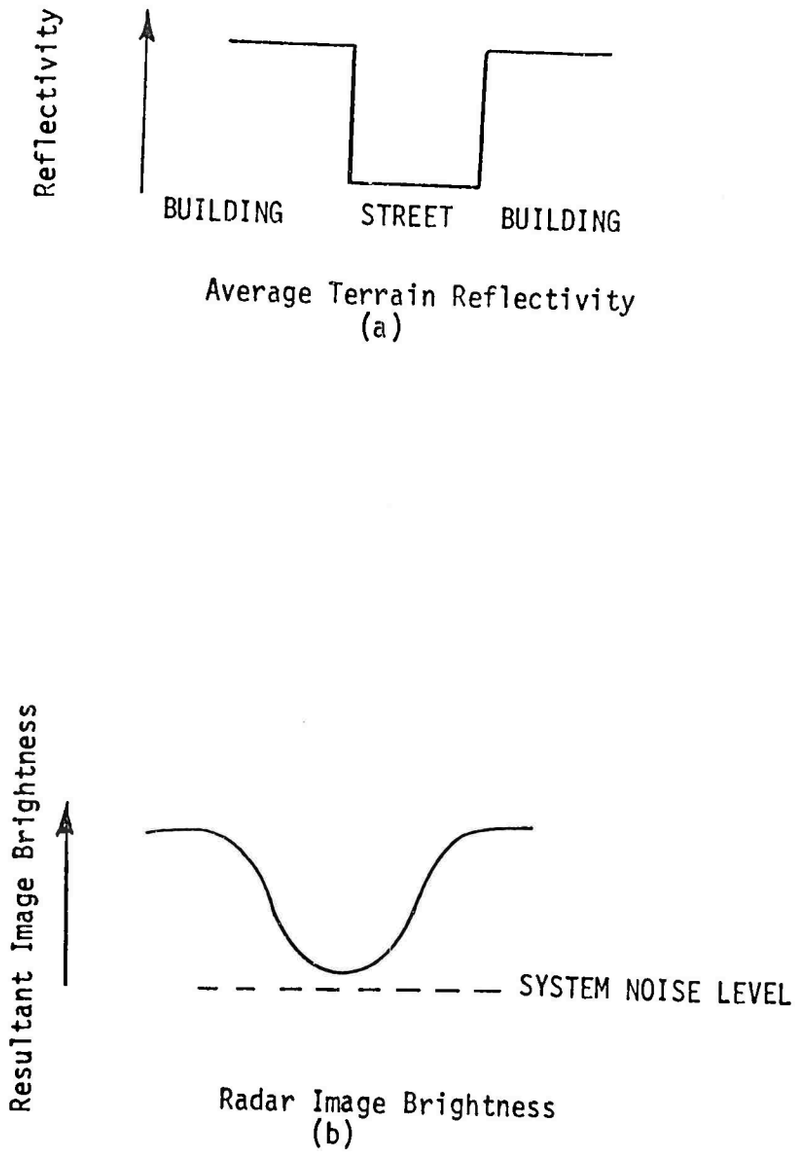

Figure 21. Response to Terrain

radar image brightness resulting. Here, the contrast (brightness ratio of buildings-to-street on the image) is very nearly the ratio of mainlobe-to-sidelobe energy.

So far, then, image quality is intuitively related to the impulse response width, sidelobe levels, and ratio of mainlobe-to-sidelobe energy. In principle, the suppression of sidelobe responses can be attained by means of weighting both the synthetic aperture and the radar pulse.

4.3 Non-Ideal Imagery

In addition to the effects that an ideal impulse response has on image quality, adverse effects can occur due to non-ideal amplitude and phase variations in the system, and due to dynamic range limitations.

Phase and Amplitude Error Effects

Figure 22 shows how the actual amplitude and phase of a signal can deviate from ideal. Amplitude and phase errors that vary rapidly across the pulse (frequency) bandwidth will perturb the impulse response in the range dimension. Those errors that vary rapidly across the doppler bandwidth will perturb the impulse response in the azimuth dimension. Similar effects upon range and azimuth sidelobes result from temporal amplitude and phase fluctuations which are rapid compared with the uncompressed pulsewidth and the time required to fly an array length. Figure 23 shows the effect on the range or azimuth impulse response of an amplitude error composed of two sinusoidal components each completing more than one cycle per bandwidth. The paired echoes resulting from this gain error

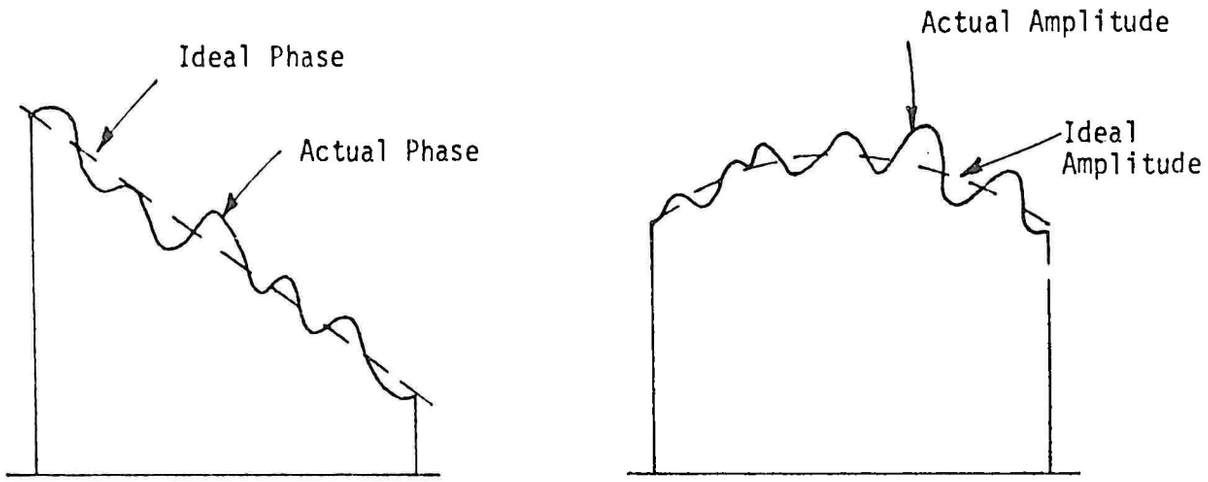

Figure 22. Phase and Amplitude Errors for a Linear FM Signal

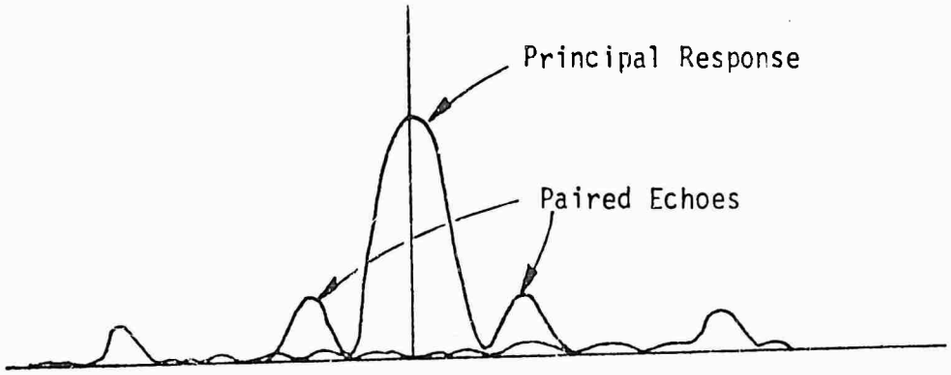

Figure 23. Effects of Two Sinusoidal Amplitude Errors

raise the sidelobe level and the total sidelobe energy. A gain error with less than one cycle per bandwidth would degrade the impulse response width.

Some causes of gain errors are: variations in transmitter power during a pulse (or pulse-to-pulse); amplitude ripples across amplifier passbands; modulation of recording cathode ray tube beam currents; nonlinear deviations of film recorder sweeps and film transports; amplitude variations across pulse compression networks or delay lines; and analog to digital (A/D) converter comparator voltage modulation. Some causes of phase errors are: phase variations in the propagation medium; uncompensated real antenna accelerations; imperfect knowledge of radar platform speed; deviations of recorder time bases from ideal (nonlinear sweeps, film transport instabilities or trigger jitter); and A/D converter sampling time jitter.

Nonlinear Effects

Typical of synthetic array radars is a performance limitation due to finite system dynamic range which exerts considerable influence on the characteristics of the final SAR map. Dynamic range constrictions can occur in any element of the receiving system but typically occur in either the pulse compression network or the processor, or both. The upper end of the dynamic range of such devices is limited by a saturation condition and the lower end by internal noise. Two principal types of effects occur due to the intermodulation distortion and signal suppression which nonlinearities produce. The signal suppression effect is of importance when a single large scatter dominates the return. If the return is strong enough to cause saturation, low reflectivity features of interest may be suppressed down to the noise level.

4.4 Imagery Analysis/Synthesis

Prediction of the radar response to an actual complex target in a physically realistic environment is often beyond the scope of purely analytic techniques. This is due to many factors: (1) Realistic target models require a large number of individual scatterers, each of which may have a complicated nature. (2) The interaction of the environment with the target and its radar return can have a significant effect on the radar response. (For example, in the case of ship targets, the ocean environment induces ship motions which can signficantly affect the phase of the return signal. Furthermore, the roughness of the ocean surface can have an extremely important effect on the amplitude of the return signal.). (3) The complexity of modern radar systems in itself can elude comprehensive analytical evaluations even with simplified models of the target and the environment.

Simulation Example

In Figure 24, the result of a computer simulation of SAR imagery is shown. This simulation assumed a system impulse response that is typical for optical processing types of synthetic aperture radars--that is where the sequence of pulses is uniformly weighted prior to forming a coherent azimuth beam. The result is strong azimuth sidelobes for the more intense scatterers. The range sidelobes were assumed to be extremely low. The target area is a 2.25 x 2.25 mile area of North Long Beach, California. The United States Geological Survey Map for this area is shown in Figure 25 In Figure 26, is an aerial photograph of the same area. The parameters that governed this simulation are listed below:

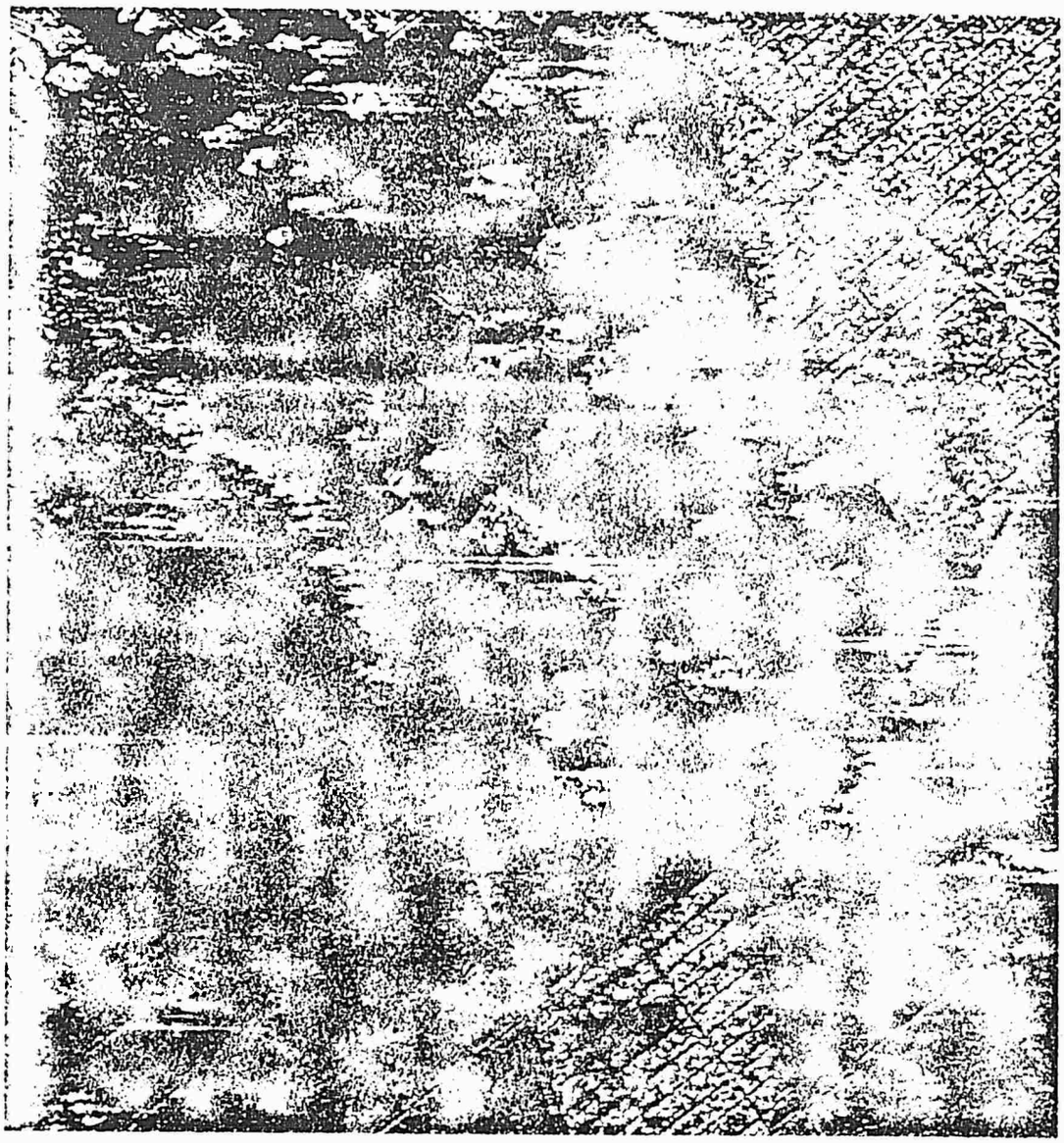

AREA = 2.3 X 2.3 MI. RESOLUTION = 20 X 20 FT. NUMBER OF CELLS = 360,000
NORTH LONG BEACH, CALIFORNIA

Figure 24. Simulated SAR Imagery of North Long Beach, California

(Film Saturation = 1)

Figure 25. Topographic Map of Target Area in North Long Beach, California

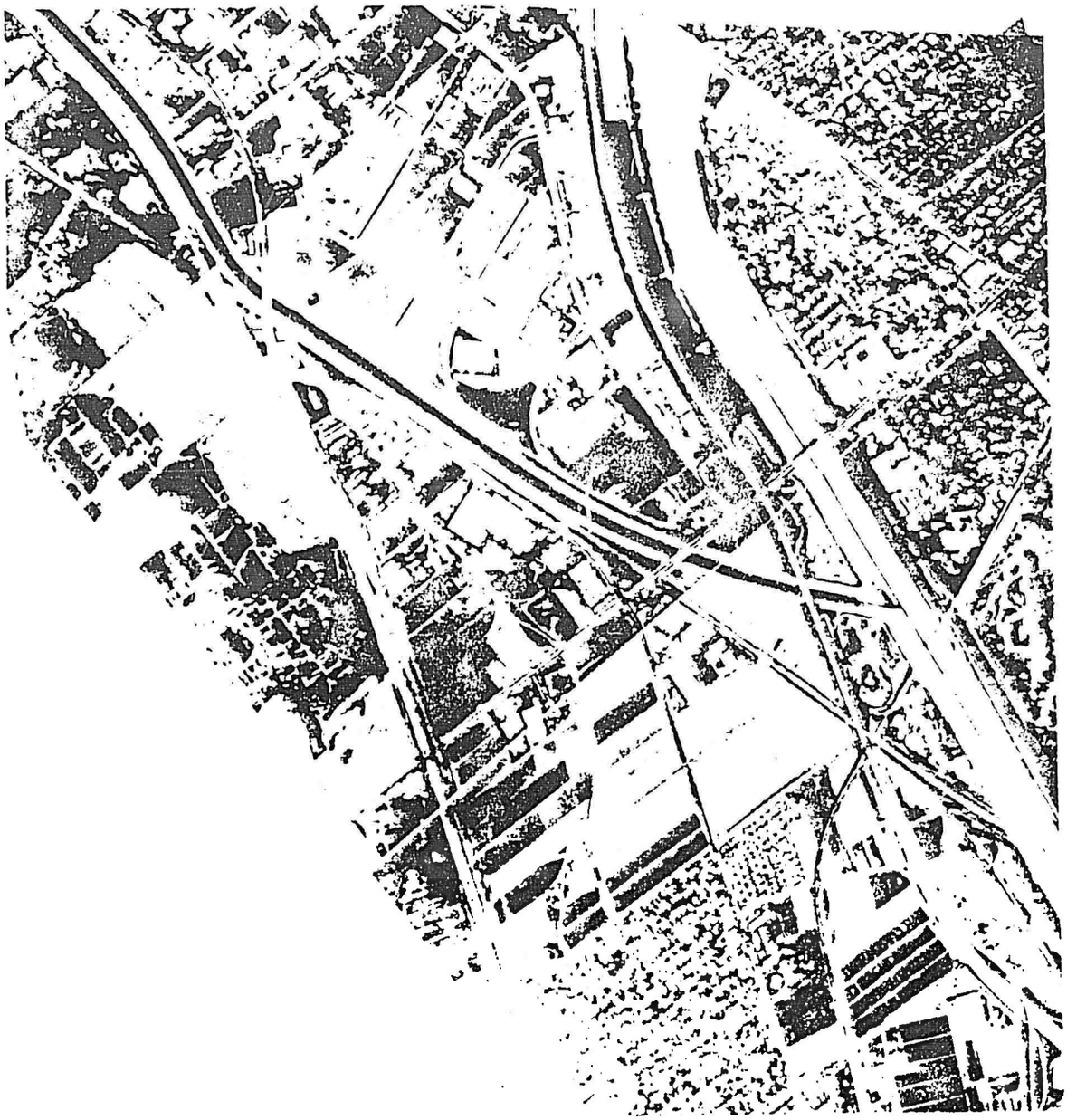

Figure 26. Aerial Photograph
of Target Area

Resolution - 20 x 20 ft

Number of cells in frame - 594 x 594

Area of frame - 2.25 x 2.25 mi

Depression angle of radar - 5 deg

Azimuth angle of radar - 38 deg (east of north)

Cell fluctuation - Rayleigh amplitude (single look)

No nonlinear effects were simulated.

A detailed analysis of this image shows that, for the natural terrain, the key features are the bright return on the leading edge of the hillside (the radar is located at the top of the figure) and the W-shaped shadow zone near the Borrow Pit. There is no return from the Los Angeles River nor the Compton Creek. The two residential areas show an increased brightness of about a factor of two from the surrounding natural terrain. The strong returns where azimuth sidelobes are evident are from bridges and transmission towers along the Los Angeles River and from the oil storage tanks on the left hand side of the image. Although not shown here, the effect of increasing the film saturation level in steps of a factor of two is to make the low-level background less visible while at the same time retaining the strong responses from the more intense scatterers.

The data based used for this simulation consisted of the following elements within the target area:

45 terrain contours
2 rivers
80 buildings
30 transmission towers
6 bridges
30 oil storage tanks
50 roads

2 freeways
1 major boulevard
4 railroad lines with multiple spurs
1 train
3 trailer parks
5 parking lots

Special Effects

There are a number of special effects that cause difficulties in visual SAR image interpretation. These effects include the following:

- large dynamic range
- non-intuitive coordinate system of delay and doppler
- multiple scatterers within a single resolution cell
- coherent image breakup and large statistical variations
- target reflectivity at radar wavelengths
- multiple images due to multiple reflection paths
- target return affected by surrounding "ground" plane
- special geometries (e.g., small trihedral corners cause large returns)
- directional scatterers causing extremes in returns depending on orientation
- doppler response of moving targets
- sidelobes of system impulse response

An untrained analyst of SAR imagery would naturally depend upon the intuition that he has gained through everyday visual scenes. This intuition is based upon a geometric system of elevation and azimuth angles. However, in the range direction of SAR imagery (even if corrected to ground range) mappings must be non-intuitive. Suppose, for example, that there is a very tall building with a corner reflector on its roof (see Figure 27). And suppose that the direct reflection back to the radar from the side of the building is of low intensity

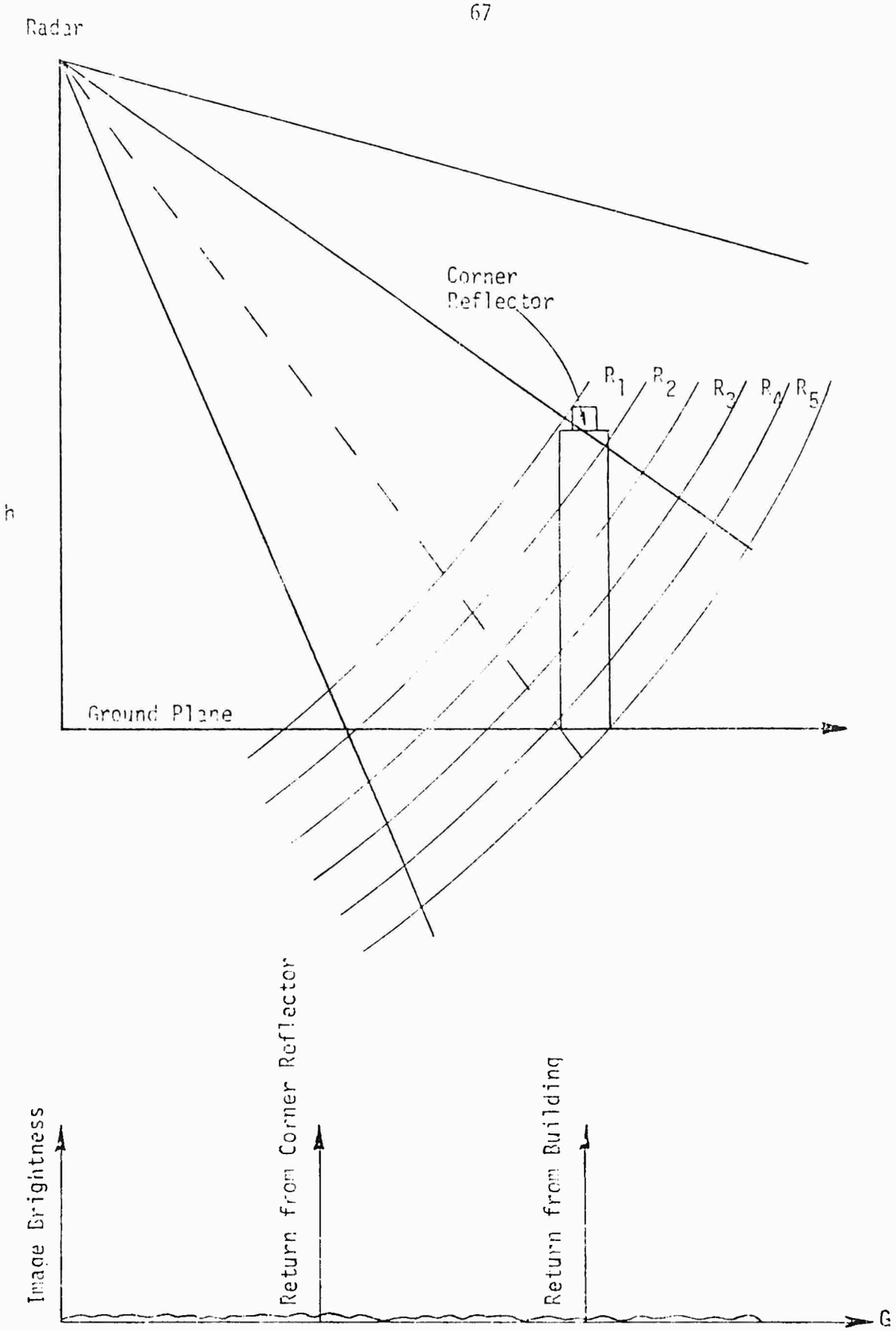

Figure 27. Illustration of Lay-Over Effect

compared with that of the corner reflector and the multiple reflection involving the building side and the ground plane. It can be shown that the two-way range and, therefore, the delay of each such multiple reflection is equal to the delay of the intersection of the building side with the ground plane. Thus, the intensity profile in ground range for this building could appear as two distinct strong returns--one at the ground range of the building and another at a ground range several resolution cells in front of the building.

Differences between radar wavelengths and optical wavelengths also cause difficulties in image interpretation. In contrast to SAR images, everyday visual scenes exhibit a rather limited range of intensities and each distinct surface appears to be fairly uniform in brightness. Whereas, in the case of SAR imagery, an extreme range of image intensities and severe coherent image breakup are commonplace. These differences are due, in part, to the much longer wavelengths in the radar, where surfaces are effectively smoother than at optical wavelengths. In addition, the illumination on surfaces from natural sources is noncoherent. This noncoherence causes visual scenes to appear more uniform than SAR imagery.

In the case of moving targets, their SAR images may appear to be either distorted or smeared in the azimuth (doppler) direction. Since SAR systems map the reflected returns from scatterers into range-doppler space, rotational target motions will perturb the doppler frequency of the radar return from each scatterer. If a scatterer is moving toward the radar with constant velocity (during the time required for formation

of the synthetic array), then its return will be displaced in the positive doppler direction such that its relative location appears translated. Conversely, if a scatterer is moving away from the radar, then its return will be translated in the negative doppler direction. Thus, a target image could appear to be either stretched or reversed in the doppler direction, depending upon the sense of the rotational motion.

If a target is moving either away from or toward the radar with a constant acceleration (during the formation of the synthetic array), then its return will not only be displaced, but it will also be dispersed over a doppler extent that is proportional to its acceleration. This effect produces an image that appears smeared or out of focus.

On large, complex targets composed of hundreds or, possibly, thousands of scattering centers, slight angular rotations of pitch, roll, and yaw can cause a wide range of doppler shifts and doppler dispersions associated with the 3-dimensional geometric distribution of scatterers. Thus, visual examination of such images usually results in poor target recognition performance.

4.5 Summary

In this section we have discussed the physical characteristics of optically processed SAR imagery. Imagery resulting from both ideal and non-ideal radar performance was discussed. Causes of non-ideal imagery are due, in general, to phase and amplitude errors and limited dynamic range. A detailed account of imagery analysis and imagery prediction (i.e., synthesis) was given. An example of a computer simulation of SAR imagery was

presented for a 2.25 mi x 2.25 mi area of North Long Beach, California. Special effects which cause difficulty in visual SAR image interpretation were discussed. These effects include non-intuitive mappings to SAR space. apparent surface roughness at radar wavelengths, and moving targets.

5.0 IMAGERY INTERPRETATION AND SIGNATURE ANALYSIS

Except in the case of change detection, the traditional approach to analysis of synthetic aperture imagery has been visual interpretation. This approach requires that the objective of SAR data processing be the formation of "recognizable" images. There is a fundamental problem associated with this approach, as discussed above; namely SAR images are highly non-intuitive. The table below summarizes typical differences between SAR imagery and common visual scenes through which human intuition is developed.

Characteristic	SAR Imagery	Visual Scene
Intrinsic Dynamic Range	60 dB	20 dB
Geometric System	Delay vs Doppler	Elevation vs Azimuth
Mapping from 3-D	Many-to-One	One-to-One
Nature of Visual Stimulus	Coherent Image Breakup	Diffuse Uniform Objects

The visual interpretation approach has been hampered by a second fundamental problem; namely, insufficient samples of SAR imagery. Large numbers of SAR imagery are required in order to gain a comprehensive understanding of the nature of the imagery and how it may best be utilized to provide intelligence. There are several reasons for this situation, not least of which is the high cost of building radars, performing flight tests, and processing images. However, there are other severe technical limitations. For example,

the very high-dimensionality of the data space: An SAR image can vary significantly from cell to cell, as well as over small changes of aspect angle, depression angle, environmental conditions, and target type.

There have been some advances to alleviate this problem, however. One advance was discussed in Section 3.3, namely, the use of frequency diversity; but as pointed out in the discussion, it is very costly to build and maintain a frequency agile radar system.

Other approaches may also be considered. These alternate approaches include: (1) the application of classical and empirical statistical methods, (2) the application of modern data-analytic techniques, as in pattern recognnition, and (3) the use of radar target simulators to generate a large number of image samples at low cost. Before discussing these new approaches, it should prove enlightening to the reader to consider the problem of visual interpretation and analysis.

5.1 Visual Interpretation and Analysis

At the outset of a visual analysis of SAR imagery one is faced with a number of questions, namely:

- how does one get oriented?
- can distances in radar imagery and ground truth be scaled accurately for correspondence?
- which types of scatterers appear brighter than the surrounding regions?
- can outstanding features be accounted for?

- Why, for certain types of scatterers (e.g., roads), do some sections appear brighter than other sections?
- what causes the fine structure observed in the radar imagery?

The following is a discussion of a visual analysis of actual imagery that addressed these and other related questions.

General Considerations

Linear features of long extent in radar imagery appear to be the best features with which to orient oneself. In particular, the radar image of a road, especially if it is bright, can serve as a good reference. The intersections of roads provide landmarks with which to locate individual scatterers. In rural areas, trees can appear much brighter than the surrounding fields; this effect is greatly enhanced when the trees are arranged in a lineal pattern, e.g., along roadways.

Scaling directly between radar imagery and ground truth is usually sufficiently accurate for purposes of orientation; however, it may not be accurate enough for locating individual scatterers, especially when scaling over large distances. In one case of imagery analysis, 30% errors were encountered when measuring over large distances. (Investigators familiar with this particular imagery attributed the lack of scaling to the flight path meandering and the nonprojective nature of synthetic aperture imagery.) Therefore, individual scatteres must often be identified in the radar imagery by the imagery pattern in its immediate vicinity.

In addition to trees appearing bright in rural areas, man-made structures, such as oil pumps, isolated buildings, and reservoirs appear bright, as well. Certain acreages appear bright in contrast with other acreages. Residential areas generally appear brighter than surrounding areas without buildings. Within regions of developed land, trihedral geometries seem to account for many of the brighter outstanding regions.

Several anomalies do occur in the radar imagery, some of which can be easily accounted for. Others require further detailed investigation and detailed computations, or a more complete description of the scatterers.

Fine structure may appear in the imagery and warrant special consideration. Various parameters may have a bearing on the appearance of fine structure. These parameters would include the following: radar resolution, sensitivity of radar imagery, relative orientation, size and spacing of scatterers, coherency of scatterers, and wavelength. Peculiar "false resolution" effects appear to be common for targets having detail which is smaller than one resolution cell since they may induce fine structure ("can of worms" effect) into the imagery through mutual interference.

Signature Analysis

Detailed signature analysis can be very difficult and tedious for an unaided human interpreter. Even the best trained interpreters face the problem of an insufficient data base. He may learn the details that characterize the signature of particular targets under certain conditions, but when the conditions are changed from those with which he has become familiar (e.g., a change in orientation) he usually has difficulty

with target identification. Sometimes, even if the target orientation is changed only slightly, he may have great difficulty because the coherent breakup may significantly alter the spatial distribution of intensities.

The use of diversity, i.e., changing the carrier frequency from pulse to pulse, and incoherently summing the images resulting at each frequency (as discussed in Section 3.3) can, in some cases, provide tremendous assistance to the interpreter. In effect, it reduces the variance of target signatures and provides an estimate of the ensemble average signature for analysis. Figure 28 shows examples of simulated single frequency, single pass SAR images of a ship. (The simulated radar is located at the top of the frame in each case; and the picture coordinates are slant range versus azimuth.) Figure 29 shows the corresponding ensemble average signatures (the limit toward which frequency diversity would tend). The pictures speak for themselves.

5.2 Background of Statistical Theories of Radar Imagery

In many applications the amount of data to be processed, even if it is formed from multiple frequencies, would overwhelm the visual SAR analyst. Under such circumstances, we would logically look to statistics for a tractable solution. Furthermore, statistics have been used very effectively in other radar system analyses.

Twenty-five years ago a great advance was made in understanding the performance of detection radars. This advance was brought about by the formulation of the problem of detection of a target by a radar as a classical statistical hypothesis test.[5] This formulation involved

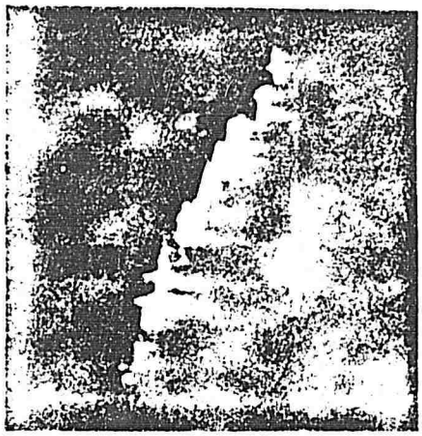

(a) Pass 34

(b) Pass 36

Figure 28.

Single Sample Images at
Two Different Headings

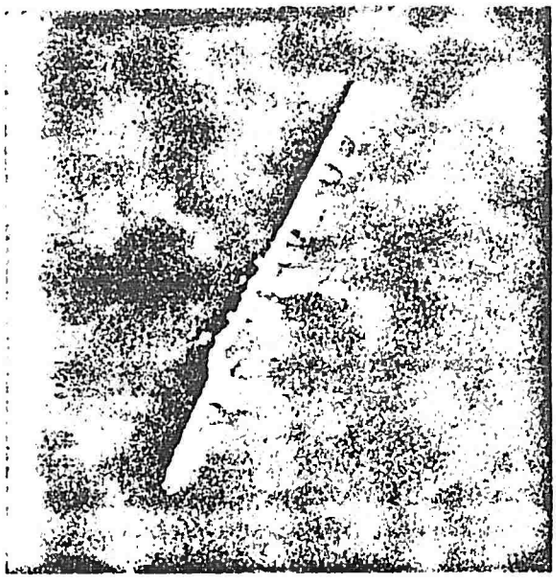

(a) Pass 34

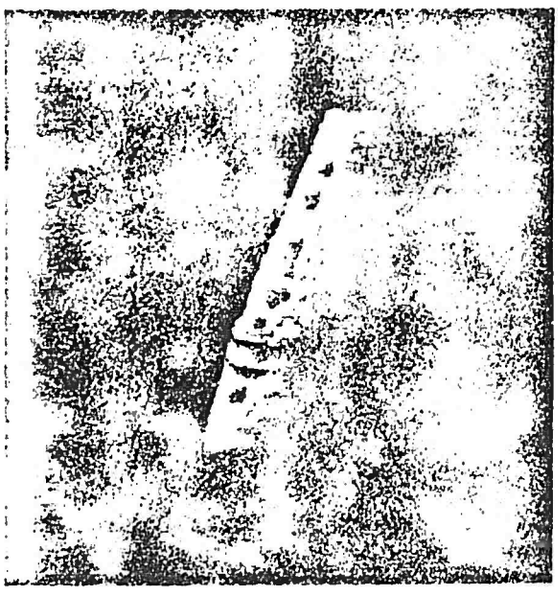

(b) Pass 36

Figure 29.

Ensemble Average Images

a number of idealizations. Nevertheless, it provided a sufficiently good representation of the real-world detection problem as to prove enormously useful in predicting radar detection performance and in delineating the dependence of performance on system, target, and environmental parameters.

Because of the success of a statistical approach in the radar detection problem, the question has often been raised as to whether a statistical theory can be developed for imaging radar performance or radar image interpretation. Such a theory would be expected to include hypothesis testing or estimation problems which are sufficiently tractable to be solved and at the same time sufficiently realistic as to be useful.

Limited progress along these lines has been made for specialized imaging problems, particularly by Develet.[6] Develet's treatment involves considerable idealizations of system characteristics, and target reflection statistics. However, the main limitation to his approach seems to be that only rather specialized image interpretation problems appear to be amenable to formulation in this manner.

To illustrate, Develet considered the following problem: Suppose the target field consists of two regions, R_1 and R_2. In both regions, the scattering mechanism consists of many small scatterers with relative phases which can be considered random (it is supposed that even the smallest resolution cells under consideration contain many such scatterers). Regions R_1 and R_2 differ in that the average reflected power per unit area is different in R_1 and R_2. (A special case is that one of the regions has zero average reflected power per unit area.) Because of the assumed nature of the scattering

mechanism, the imaging radar output amplitude in each resolution cell will be Rayleigh-distributed, and the power will have an exponential probability density function (See Appendix A.)

Develet considered the problem of detecting Region R_2 (i.e., testing the hypothesis that there is only one region) as well as of estimating the location and width of Region R_2, in cases where Region R_2 has very simple shapes: for instance, if the boundary is a straight line, or if R_2 consists of a strip of constant width. He analyzed the effect of the imaging radar resolution as well as the effect of the number of diversity samples.

F.3 A General Statistical Formulation of Some SAR Problems

Let us now turn to a general statistical formulation of SAR problems. The following is a simplified translation into statistical terms of the SAR data available for processing, the distribution of the data, and some of the problems that need solution.

The Statistical Model

The area scanned is broken up into resolution cells $C_i, i=1,\ldots,n$, where n is large. During the time period of the scan, the SAR produces M samples of the amplitude of radiation scattered from each cell. M is small, being typically either one (if there is no frequency or angle diversity), or between one and ten. Denote these values by $\underline{x}(i) = x_1(i),\ldots, x_M(i)$ where i designates the data for the C_i^{th} cell.

If the C_i^{th} cell contains many small scatterers with random relative phases, then it can be shown that the $x_1(i),\ldots, x_M(i)$ are independently drawn from an underlying Rayleigh distribution provided the changes in angle

or frequency are sufficiently large. (Otherwise, $x_1(i),\ldots,x_M(i)$ will be correlated to some extent.)

This will be the case if, for example, the C_i^{th} cell consists of a heavily foliated region, a meadow, a dirt field with a rough surface, etc. Regular topographical features and man-made objects will produce a different statistical distribution for $\underline{x}(i)$. For instance, one large reflector and a number of small randomly oriented reflectors in a cell will lead to a Rice distribution (see Appendix A). The returns from a highly directional reflector will tend to have a log-normal distribution. In addition, if the assumptions leading to the Rayleigh distribution are violated, then the readings $x_i(i),\ldots,x_M(i)$ may have a definite dependency.

The assumption is usually made that the sampling in each resolution cell is independent of the sampling in the other cells. To estimate the mean of a Rayleigh by maximum likelihood, under this assumption, one should use the estimate

$$\frac{\sqrt{\pi}}{2}\left(\frac{1}{M}\sum_{1}^{M} x_j^2(i)\right)^{1/2}$$

In other words, use an estimate which is a multiple of the RMS power. In this latter case the estimate would also have a standard distribution, being essentially the square root of a X^2 distribution with 2M degrees of freedom.

In any case, we take our statistical model to be defined by

a. The n vectors $\underline{x}(i),\ldots,\underline{x}(n),\ldots$ corresponding to the n cells are mutually independent.

b. The sample of M values $x_1(i),\ldots$ comes from the same underlying probability distribution P_i but may be dependent. The underlying distribution P_i is unknown.

In the above form the model is too general to do much with and additional assumptions concerning the P_i will have to be made. In the following we outline the statistical/data analytic problems involved in analyzing the data and remark on some plausible additional assumptions that will make the problems specific enough to be solved.

The Problem Areas

The basic problem breaks down into three parts, all of which can be described in standard statistical terms:

a. Is something there? I.e., has some change occurred?

   Statistical Problem: Hypothesis Testing

b. If there is something there, where is it?

   Statistical problem: Estimation

c. Now that it has been located, what is it?

   Statistical Problem: Classification/Pattern Recognition.

The first two parts of the problem are quite similar to a much simpler but well known statistical problem that is common in such areas as quality control: Given a sample $x_1,\ldots,x_N$, "has something changed?" translated into: Test the hypothesis that the $x_1,\ldots,x_N$ are independent samples from the same distribution function $F(x)$ versus the alternative hypothesis that there exists a j, $1\leq j<N$ and a distribution function $G(x) \neq F(x)$ such that $x_1,\ldots,x_j$ were sampled independently from $F(x)$ and $x_{j+1},\ldots,x_N$ from $G(x)$. Usually $G(x)$ is taken to be a shift in location of $F(x)$, i.e., $G(x) = F(x+\Delta)$.

The question "where is it?" translates into: given that a change from the distribution F(i) to a different distribution G(i) occurred someplace between the first and last sample where did it occur?

The analog of the third question in a quality control background would be to characterize the type of change. That is, assuming F(x) is known and G(x) unknown, characterize the way in which G(x) differs from F(x) in a way that corresponds to a recognizable malfunctioning.

Is Something There?

One simple (in fact, usually too simple) formulation of this is to test the hypothesis that all samples in all cells are independently drawn from the same Rayleigh distribution versus some class of alternatives. For instance Develet[6] has discussed the class of alternatives in which the cells are divided into two regions R_1, R_2 by a simple boundary and the samples in R_1 and R_2 are independently drawn from Rayleighs but with common mean in R_1 differing from the common mean in R_2.

It is important to recognize when the underlying cell distribution(s) are not Rayleigh. This usually signals the occurrence of some unusual topographical feature or of a man-made feature. Since M is small, it is probably not possible to test for this on a cell-to-cell basis unless the underlying distribution differs radically from the Rayleigh. But grouping together only a small number of adjacent cells, say 10, would increase the sample size enough to give discrimination capability between a Rayleigh and a log normal, or a Rice distribution that was sufficiently non-central.

One natural problem that should be feasible to solve fairly quickly is the design of an algorithm that will test grouped data for Rayleigh versus alternatives and be computationally very efficient. This last factor is

important, since the number of cells n in each area surveyed is very large.

Notice here that using either the cell averages or pooling the M readings into any other single estimate of the mean of the cell distribution destroys valuable information as far as testing hypotheses concerning the cell distributions.

Actually, the test we are looking for should detect two things:

1. Departure from the Rayleigh distribution.
2. A change from one underlying cell distribution to another (including simply a change in mean values).

A test that simply detects departure from Rayleigh will not generally be efficient in detecting change. For example, in the model that Develet proposed, the only groups of cells that show any departure from a Rayleigh distribution are those groups that include cells from both regions. For these groups the underlying distribution would be a superposition of two Rayleighs with different means. This latter distribution is difficult to discriminate from a pure Rayleigh unless the means are quite different or the sample size is large.

Where Is It?

If an effective procedure as outlined above is constructed, then the outputs of the algorithm will also contain crude location information. It is crude in that in order to test the hypothesis in question, adjacent cells have to be grouped together. Therefore, if there is a sharp change, for instance, as from a meadow area to a highway, the change may not be picked up until the center cell is over the middle of the highway.

But once it is known that a change occurred in some small region, then estimates of the demarcation between the types of underlying distributions can be considerably refined.

As a simple model, consider the problem stated this way: consider all the cells in region R_1 have an underlying distribution $F(x)$ and in R_2 the distribution $G(x)$ and both $F(x)$ and $G(x)$ known. Assuming that the boundary between R_1 and R_2 is continuous, form an estimate of the location of the boundary. Although this model appears simple, it is not unrealistic. From the hypothesis testing stage we should be able to localize a region of change so that we are investigating only a small subarea that hopefully contains only two fairly homogeneous regions separated by a boundary. By assuming that the underlying distributions are one of a small class of families, i.e., Rayleigh + lognormal + Rice, we should be able to test to see which family provides the best fit and to estimate any parameters necessary.

As is commonly known, the one-dimensional analog of this problem is well developed; it has been extensively studied and numbers of articles related to it are known in the literature. Effective procedures are available for estimating the change points. The two-dimensional version of the problem should certainly not be intractable.

The output of this second estimation stage is therefore a subdivision of the surveyed area into subregions such that in each subregion the underlying cell probabilities are roughly equal. (Actually, this needs some qualification. As with a tract of houses, one would not necessarily want to estimate the boundary around each house, but probably the boundary around the tract or perhaps the boundaries around each block of houses).

What Is It?

Assuming that the estimation problem has been solved, we now have a number of subregions marked out, we have estimates for the boundaries and for the underlying cell distributions in each subregion.

Now the problem is: find all subregions corresponding to a given class of objects. In this form, the problem may be insoluble at present unless the class of objects specified can be effectively defined. For example, one problem that is potentially soluble is to find all subregions corresponding to linear man-made objects. Because of statistical fluctuations, probably none of the subregions produced by the estimation phase would be exactly linear. A certain amount of noise would be superimposed on the estimate. Therefore, the statistical approach would use some measure of departure of the subregion from straightness and devise a test of the hypothesis that the original "true" subregions was a linear object.

Even more complex sets of objects could be identified if modern data-analytic methods of pattern recognition were applied[23]. For example, typical features of cell distributions and subregion shapes corresponding to topographical features such as rivers could be derived. However, notice that this approach differs from that in which the question is asked: What is everything in the picture? This is a much more difficult question, because there are a virtually infinite variety of objects in the world. From a statistical, data-analytic viewpoint, the question that might be possible to answer is:

Is one of the following J classes of objects in the area?

1. straight line man-made
2. river
3. ....

.

.

.

J

In the brief summary above, we have tried to indicate some of the areas in the use of SAR which seem amenable to solution by a data-analytic statistical approach. There is evidence that many promising results can be produced by exercise of technique and ingenuity.

Some Limitations of Idealized Statistical Models

Let us now discuss in turn some of the idealizations involved and the prospects for generalizing a statistical approach.

First of all, some of the idealizations that are typically made regarding the radar characteristics are for mathematical tractability and cannot really be considered limitations in principle. For instance, in one of his problems Develet assumed a step-function type of antenna pattern.

Second, the assumption that the reflections from each region arise from many small scatterers in random phase is an idealization which is good for some types of regions (e.g., heavily foliated terrain) but can be very poor for others (e.g., terrain with many man-made features). This is a more troublesome limitation. However, the same basic approach could be applied whenever the electromagnetic scattering mechanism is such that the

statistical distribution of radar outputs for each resolution cell can be approximated by some reasonably convenient closed-form distribution. There are several families of distributions (e.g., log-normal, Rice, gamma, Weibull) which have been found to approximate the statistics of fairly varied types of target fields. The mathematics might become considerably more difficult, however.

The most intractable of the limitations is that this approach seems feasible only for very specialized types of image detection or estimation problems, typified by those described above, where the total class of possible target fields is severely restricted (e.g., to simple homogeneous regions separated by very simple types of boundaries).

In this respect, the problem of formulating a statistical theory of radar imagery interpretation does not differ from that for other types of image interpretation, e.g., photo-interpretation. Most studies of the interpretability or "quality" of, say, photographic or television imagery, and the dependence of image quality on parameters such as resolution, dynamic range (number of gray levels), etc. are performed by experimentation rather than by theoretical prediction from statistical estimation theory. The case of radar imagery is even more complicated because more parameters are involved, e.g., number of diversity samples, the fluctuations of the images, etc.

However, there are as-yet-unexploited possibilities for treating the problem of radar imagery, and extracting more information from radar imagery even in complex target situations which are typical of the real world; these

possibilities lie in the domain of modern data anlaysis techniques, particularly nonlinear pattern classification and recognition.

5.3 Application of Modern Data Analysis Techniques to Radar Imagery

It is proposed that a major avenue for possible advances in extraction of information from radar imagery would be to apply modern computer-based techniques of feature extraction and pattern classification directly to the radar outputs; and in the case where diversity is employed, such techniques should be applied directly to the samples prior to averaging. This does not of course preclude parallel processing by the more conventional techniques. (Certainly averaging is one of the useful things that can be done with diversity samples.) In this way, features of radar imagery such as fluctuations which are usually regarded as obstacles to extraction of information can potentially be converted to contributors of additional information.

Use of Simulated Radar Imagery

In order to provide statistically significant numbers of sample imagery would require a massive flight test program and development of a massive SAR imagery data center for full utilization of the acquired data. But, as is typically the case, these data would probably be of limited value since they would be restricted to the radar parameters and flight test conditions available. Furthermore, auxiliary data that could be very important to subsequent analyses would most likely not be recorded or measured. An example of such auxiliary data might be precise values of radar/target encounter geometry; or, as in the case of ship imagery, a reliable estimate of sea state (i.e., ocean waveheight).

A solution to the problem of acquiring perfectly controlled SAR data in large numbers is to generate validated simulations of SAR imagery. With such a capability, the requirements for real SAR data would be modest--real data would be used primarily for sample point tests, and the cost of SAR imagery simulation would be orders of magnitude less than the cost of collecting real SAR images.

General Approach

The general approach that would be taken in the application of modern data analysis techniques is as follows:

1. Study the system context, i.e., the system objectives and constraints.
2. Define the problem, e.g., formulate hypothesis to be tested.
3. Determine the quantity and nature of the sensor data (real or simulated) available for each of the classes of objects or processes for which a decision algorithm is to be designed.
4. Define "heuristic features" of the raw sensor data. A "feature" is a functional transformation of the sensor data which is designed to summarize or emphasize some aspect of the original data and which is statistically different for objects from each different class. Thus, it is also a candidate discriminant. A "heuristic feature" is one which can be postulated a priori either because it is motivated by physical principles or because it is suggested by the analyst's review of portions of the sensor data. An example of an "heuristic feature" is the mean value of the radar cross section in each SAR resolution cell. The value of a feature for a given set of conditions may differ significantly (in a statistical sense) from one target type to another.

5. Automatically derive "objective features". "Objective features" are functional transformations of the raw data as were the "heuristic features". The principal difference is that the transformation is parameterized and the parameters can often be subsequently specified by an optimization procedure involving the data itself. This technique adds strength to the analysis because feature generation is no longer dependent upon either the existence of a body of physical theory about a process or the somewhat dubious assumption that a human, viewing a small portion of the relevant data, can "recognize" statistically valid, high-information content features.
6. Automatically rank single features and groups of features and select the sets of features which jointly possess the highest information content for the detection or classification objective specified. The selection of the highest information content features amounts to a third transformation which selects P features from a set of K features (heuristically or objectively defined). This transformation can be represented as a special matrix product of the K dimensional feature vector (see Figure 30). That is,

$$\underline{x} = [S]\,\underline{y}$$

where $\underline{x}$ is P dimensional, $\underline{y}$ is K dimensional, and [S] is a special selection matrix of dimension PxK made up of "1"; s and "0"'s; a single "1" per row, and no more than a single "1" per column.

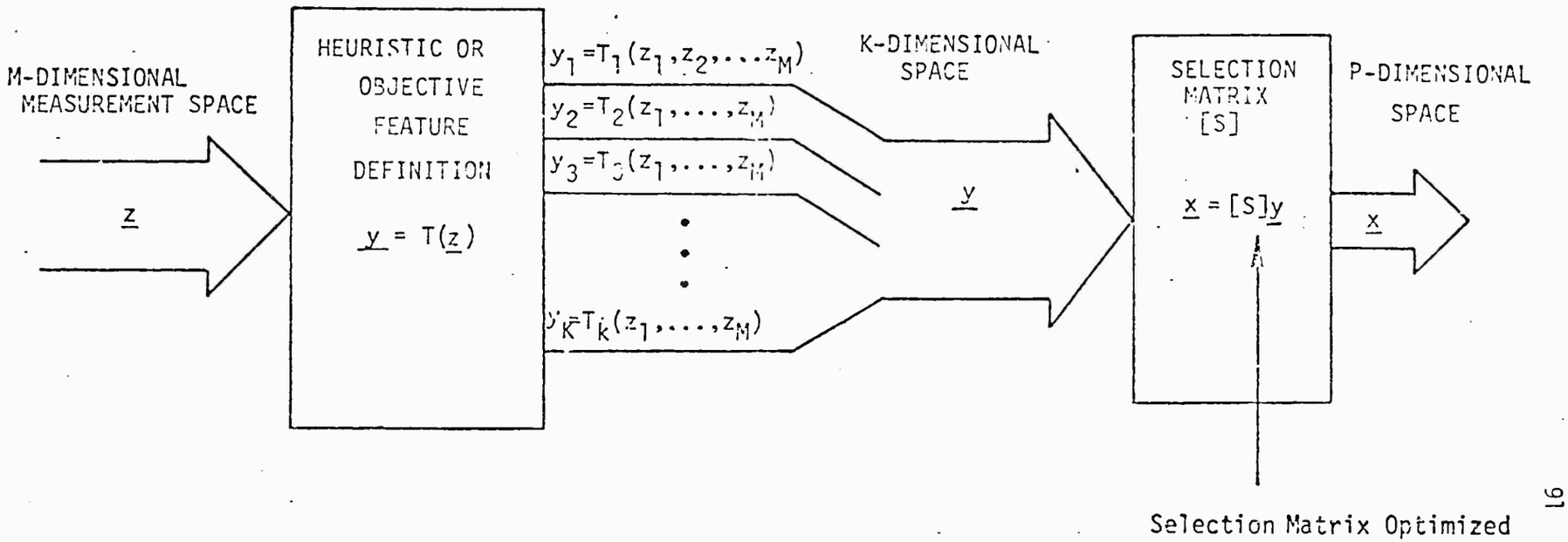

The PXK dimensional selection matrix maps the K-dimensional feature space into a P-dimensional space made up of a selection of P of the K features.

e.g., P=3
K=8

$$[S] = \begin{pmatrix} 1 & 0 & 0 & 0 & 0 & 0 & 0 & 0 \\ 0 & 0 & 1 & 0 & 0 & 0 & 0 & 0 \\ 0 & 0 & 0 & 0 & 0 & 1 & 0 & 0 \end{pmatrix}$$

$$\underline{x} = [S]\underline{y} = \begin{pmatrix} y_1 \\ y_3 \\ y_6 \end{pmatrix}$$

Figure 30. Feature Selection Optimization

7. Develop a decision algorithm based on the selected features which is highly reliable. It must also be highly efficient when there is requirement for efficiency because of real-time constraints of the system environment.

8. Estimate the performance (validity) of the decision algorithm based on independent test data and statistical tests.

The foregoing steps would generally be applicable to any of the several problem contexts. Beyond step 3 the procedure is almost entirely objective and thus problem-independent, thereby making it possible to develop a single body of techniques that can be applied to a broad spectrum of problems.

Although all of the foregoing steps are of vital importance to the ultimate success of a detection/discrimination project, perhaps the key step is that of feature creation -- the definition and derivation of high information content features. It is this step which intrinsically defines an upper limit on the ultimate performance of any resulting discrimination system.

Paradoxically, this step has in the past not been approached systematically. Where resources have been applied to the feature creation task, they have been predominantly allocated to examination in detail of single heuristic features. This is probably due to the fact that powerful, highly general methods of deriving objective features and systematically comparing heuristic features have only recently come into use. Figure 31 shows a flow diagram of a systematic approach to objective feature creation and feature selection. For the classification problem, these techniques are usually found in the literature on "pattern recognition" [23].

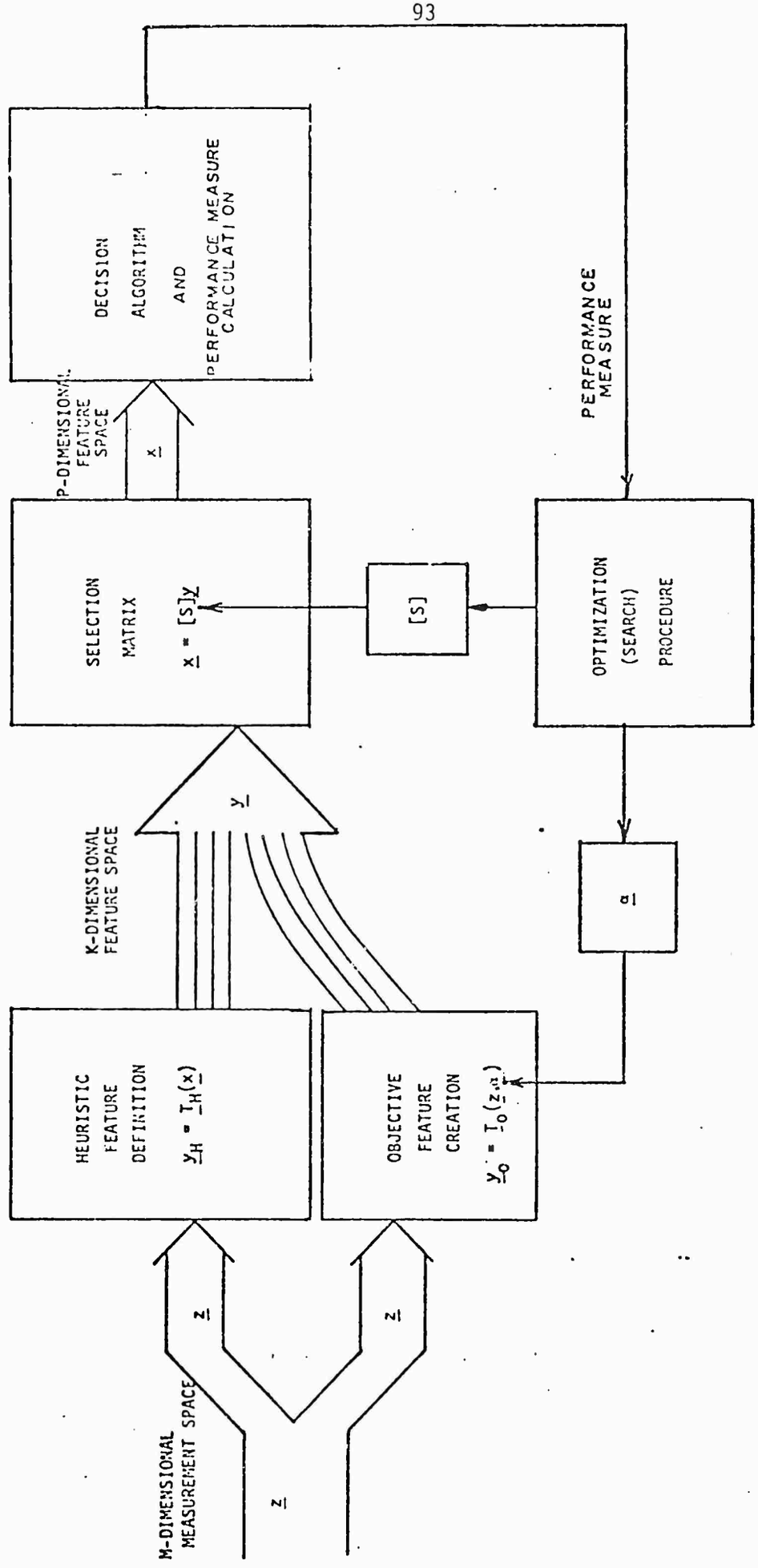

Figure 31. A General Feature Creation/Selection Procedure

5.4 Recommended Areas for Further Study

In general, areas for further study by statisticians should involve the determination of useful statistical descriptors for both the temporal and spatial properties of high-resolution SAR imagery. This should be done from two points of view: (1) theoretical, based on scattering theory adopted to the high-resolution case and (2) empirical, based on computer-based analyses of actual digitized SAR imagery.

There is a need to develop the amplitude fluctuation statistics for few or single scatterers within a resolution cell. Having the appropriate statistical models would enhance parametric approaches, including maximum likelihood methods, to quantitative image interpretation and target classification. The appendices of this report may prove useful for development of models.

Another area of interest would be compensation of target motion. Fundamentally, there are two approaches that could be taken with regard to minimizing this problem. The first is to process the data in an unconventional way in order to produce more recognizable images. (This approach has been proposed or attempted by various radar groups.) The second approach is to use the data as they exist, but perform unconventional (i.e., automated) recognition functions that do not depend upon visually recognizable images.

As examples of the first approach to the problem, one can attempt to minimize image smearing by adaptively focusing over small increments in range, thereby minimizing the number of scatterers for a given focal length. Or, one could correlate the phase histories only over portions of

the synthetic array, rather than the whole array. This technique, in effect, "freezes" the target by integrating over a sufficiently short interval in time. However, the image suffers a loss in resolution (the resolution is inversely proportional to the integration time).

As an example of the second approach, one could attempt to define characteristics of target signatures (e.g., through abstract nonlinear transformations) that would tend to be invariant with image distortions and noise. Using these transformations, one could operate on sample imagery (simulated or real) to develop a parametric classification rule that can be optimized over a wide range of conditions (e.g., over ranges of the costs of false alarms and missed detections). And, finally, test the decision algorithms on an independent set of images in a systematic fashion. (This second approach could be applied to any of a wide range of problems in target classification, not just recognition of targets in motion.)

A third area of interest for further study would be to define the statistical and deterministic properties that characterize natural backgrounds, cultural background, background targets, and targets of interest. If such properties could be defined, they would be extremely useful in filtering data of potential interest for a human interpreter. Otherwise he would have to scan huge amounts of data before encountering significant information--in this mode of operation, his effectiveness would be minimal.

5.5 Summary

In this section, we first discussed the traditional approach to analysis of synthetic aperture radar imagery: namely, visual interpretation. We have briefly described the fundamental difficulties of this approach

and have suggested alternate approaches. These alternate approaches are: (1) the application of classical and empirical statistical methods, (2) the application of modern data-analytic methods, and (3) the use of radar target imagery simulators.

The key features of visual image interpretation and signature analysis were presented. Questions of orientation, scaling, and detail characteristics of SAR imagery were discussed. In general, lineal features are useful for orienting oneself. Scaling between SAR imagery and "ground truth" (e.g., maps and aerial photography) may be difficult, at times. Relative brightness of particular scatterers was indicated. The use of frequency diversity as an aid to visual interpretation was discussed; examples of simulated ship images that are indicative of imagery with and without frequency diversity were presented.

Next, possible statistical theories of radar imagery were suggested. Simple examples of previous work done in detecting the existence and location of boundaries for statistically homogeneous regions were presented. Following this, a general statistical formulation of SAR problems was presented. First, a generalized statistical model was discussed; the Rayleigh amplitude statistical model was shown as an example. Other statistical models that should be considered include the Rice distribution, the log-normal, the χ^2, the Weibull, and the gamma. Second, an indication of how to formulate a statistical analysis problem in the SAR context was presented.

In statistical terms, the approach can be stated as a three-stage process: (1) hypothesis testing, (2) estimation, and (3) classification.

In other words, hypotheses must first be made regarding the probability distributions of random processes; then the hypotheses must be tested to detect either a change (test homogeneity) or to detect the presence of something (test consistency). Following this, the next step in sophistication is to determine where a change occurred or the extent and location of a homogeneous region. The highest level of sophistication is then to classify or identify what has been detected and located. A viable solution to this last problem requires having a prototype model or a design data set with which to perform maximum likelihood tests for classification.

Limitations of idealized statistical models were then discussed. Because of the complex nature of SAR imagery, it is felt that only very specialized types of image detection or estimation problems can be handled by strictly statistical methods. However, there are as-yet-unexploited possibilities for analysis of SAR (or other) imagery. These possibilities lie in the domain of modern data analysis techniques. (Prior work has been performed in the area of conventional linear imagery analysis however, recent developments in (1) systematizing the data analysis methodology, (2) nonlinear analysis techniques, and (3) the use of simulated data should open new avenues for research.)

An outline of the application of modern data analysis to SAR imagery was then presented. The efficacy of using simulated data was discussed, and this was followed by a step-by-step description of a systematic data-analytic approach. The most important step in the entire data analysis

process is the creation of discrimination features since the performance of classification or discrimination algorithms is intrinsically limited by the information content of the feature set.

Finally, a brief statement of recommended areas for further study by statisticians was provided. These areas are: (1) statistical modeling of fluctuations for various combinations of scatterers, (2) compensation of target motion, and (3) realistic statistical characterization of backgrounds and targets--especially for filtering out large amounts of superfluous data prior to reaching a decision point.

BIBLIOGRAPHY

1. Skolnik, M. I., editor, Radar Handbook, McGraw-Hill Book Co., N.Y., 1970.

2. McCord, H. L., "Synthetic Array Radar" -- Course Notes.

3. Rihaczek, A. W., Principles of High-Resolution Radar, McGraw-Hill Book Co., N.Y., 1969.

4. Barton, D. K., Radar Systems Analysis, Prentice-Hall, Inc., New Jersey, 1964.

5. Marcum, J. I. and P. Swerling, "Studies of Target Detection by Pulsed Radar," IRE Trans. Info. Theory, Vol. IT-G, No. 2, April 1960 (reporting earlier work at the Rand Corporation).

6. Develet, J. A., Jr., "Synthetic-Aperture Radar," TDR-229 (9990)-8, the Aeorspace Corporation, 14 August 1964.

7. Harger, R. O., Synthetic Aperture Radar Systems: Theory and Design, Academic Press, New York, 1970.

8. Cutrona, L. J., E. N. Leith, L. J. Porcello, and W. E. Vivian, "On the Application of Coherent Optical Processing Techniques to Synthetic Aperture Radar," Proceedings of the IEEE, Vol. 54, No. 8, August 1966.

9. Brown, W. M., "Synthetic Aperture Radar," IEEE Transactions on Aerospace and Electronic Systems, Vol. AES-3, No. 2, March 1967.

10. Brown, W. M., L. J. Porcello, "An Introduction to Synthetic Aperture Radar," IEEE Spectrum, September 1969.

11. Pernick, B. J., "Distortions of Synthetic Aperture Radar Imagery due to Target Motion," Applied Optics, Vol. 13, No. 3, March 1974.

12. "Technical Note: Ship Target Motion Effects on Synthetic Aperture Radar Imagery," Airborne Instruments Laboratory, Department of Radar Systems, J-0621.

13. Mims, J. H., J. L. Farrell, "Synthetic Aperture Imaging with Maneuvers," IEEE Transactions on Aerospace and Electronics Systems, Vol. AES-8, No. 4, July 1972.

14. Mitchell, R. L., "Models of Extended Targets and their Coherent Radar Images," Proceedings of the IEEE, Vol. 62, No. 6, June 1974.

BIBLIOGRAPHY (Cont'd)

15. Papoulis, A., The Fourier Integral and its Applications, McGraw-Hill Book Co., N.Y., 1962.

16. Cook, C. E. and M. Bernfeld, Radar Signals, Academic Press, N.Y., 1967.

17. Goldman, S., Information Theory, Prentice-Hall, Inc., N.Y., 1953.

18. Mitchel, R. L., et al., "Synthesis of High-Resolution Radar Systems for Display Simulation and Training," Air Force Human Resources Laboratory, AFHRL-TR-71-11, June 1971.

19. Lucero, A. B., "High Fidelity Target Modeling and Computer Simulation (U)," 19th Annual Tri-Service Radar Symposium, May 1974

20. Ament, W. S., "Toward a Theory of Reflection by a Rough Surface," Proceedings of the IRE, Vol. 41, pp 142-146, January 1953.

21. Andrews, H. C., Computer Techniques in Image Processing, Academic Press, N.Y., 1970.

22. Rosenfeld, A., Picture Processing by Computer, Academic Press, N.Y., 1969.

23. Meisel, W. S., Computer-Oriented Approaches to Pattern Recognition, Academic Press, 1972.

APPENDIX A

THE RAYLEIGH AND RICE DISTRIBUTIONS

From a given resolution cell, let the time signal returned to the radar be of the form

$$S(t) = \sum_i A_i \cos(\omega t + \phi_i)$$

where i ranges over the reflectors contained in the cell, A_i is the amplitude return from the i^{th} reflector and ϕ_i the phse of the return.

Expanding gives

$$S(t) = [\sum_i A_i \cos \phi_i]\cos\omega\tau - [\Sigma A_i \sin \phi_i]\sin\omega\tau$$

$$= U \cos\omega\tau + V \sin\omega\tau$$

By definition, the power of the return is

$$||S||^2 = U^2 + V^2$$

Assume that the phases $\phi_1, \phi_2, \ldots$ are mutually independent random variables and are also independent of the set of amplitudes $A_1, A_2, \ldots$.

If the $\{A_i\}$ are "uniformly" small, then it can be shown that U and V have a bivariate normal distribution. Assuming also that

$$\overline{\cos\phi_i} = \overline{\sin\phi_i} = \overline{\cos \phi_i \sin \phi_i} = 0$$

gives the result that U,V are uncorrelated, zero mean normal variables. Adding the condition

$$\overline{\cos^2 \phi_i} = \overline{\sin^2 \phi_i}$$

results in a common variance for both U and V. All the conditions in the two equations above will hold if we take ϕ_i to be uniformly distributed on $[0,2\pi]$. Therefore, the amplitude is the square root of the sum $U^2 + V^2$, where U,V are independent mean zero variables, with common variance. This is well known to have the Rayleigh distribution.

If there is one large reflector in the cell plus a large number of small reflectors as above, then U and V have the form

$$U = A_0 \cos \phi_0 + \sum_{i \geq 1} A_i \cos \phi_i$$

$$V = - A_0 \sin \phi_0 - \sum_{i \geq 1} A_i \cos \phi_i$$

or

$$U = \mu + U^*$$

$$V = v + V^*$$

where U^*, V^* are independent mean zero, common variance normal variables. Then $(U^2 + V^2)^{1/2}$ have a non-central Rayleigh distribution; commonly called a Rice Distribution.

APPENDIX B

STATISTICAL FLUCTUATION MODELS

It is important for purposes of radar systems analysis to have some understanding of physical scattering mechanisms which lead to given RCS* statistics, not just in the sense that a specific target is observed to have given statistics, but in a theoretical sense. Here, "theoretical" is not used in opposition to "practical"; rather, it refers to a case in which given RCS statistics can be mathematically derived from a scattering model, in the sense that Rayleigh amplitude statistics (i.e., chi-square with k=1 power statistics) are mathematically derivable from a many-scatterer mechanism. Of course, the majority of real targets are only approximations to the ideal scattering mechanisms which theoretically give rise to given distributions; nevertheless, it is necessary to understand what ideal mechanisms may produce given statistics.

The requirement for such understanding arises from those cases (which are more common than any others) in which measurement data are fragmentary or have significant gaps and in which no exact physical description of the target or target population is available. In such cases, we may wish to a) extrapolate statistical models to parameter regions where measurement data are lacking or b) hypothesize a variety of possible statistical target models.

The second point is particularly important. When data and detailed physical descriptions are lacking, the standard method of approach is to postulate a variety of statistical models which are thought to bracket the behavior of the target population of interest, and then perform radar performance analyses for a variety of such models, noting the performance sensitivity to the assumed model, attempting to choose design configurations whose performance is relatively insensitive to the statistical model, etc.

However, it is essential that the postulated models be a) self-consistent, b) consistent with possible physical scattering mechanisms,

---

*Radar cross section.

and c) consistent with such measurement data as has been observed. It is very difficult to postulate consistent models of this type without some understanding of ideal scattering mechanisms which can produce given RCS statistics.

Appendix C gives a more detailed discussion of this, with several specific examples: a) postulation of models of sample correlation and joint statistical properties with respect to time; b) postulation of models for fluctuation behavior of a target with respect to frequency diversity; and c) postulation of models for detection analysis of targets which are extended in range compared to a range resolution cell.

Each of these examples is discussed in Appendix C with respect to models calling for Rayleigh RCS statistics, Rice RCS statistics, and log-normal RCS statistics. These examples illustrate why a lack of understanding of theoretical scattering mechanisms, which can give rise to given statistics, can be a stumbling block in postulation of consistent models.

1.0 Physical Models for Rice and Chi-Square Distributions

It is of course well known that the Rayleigh amplitude distribution, i.e., the exponential power distribution (chi-square with k=1 or Rice with s=0) arises from a many-scatterer mechanism, which is defined to be a mechanism with a very large number of scatterers, no one of which ever contributes more than a small fraction of the returned power, and which have random relative phases.

A Rice distribution of radar cross section with parameters ψ_o and s arises from a scatterer with a many-scatterer component whose average RCS is ψ_o, plus a single non-fluctuating scatterer having RCS equal to $s\psi_o$. The relative phases of all scatterers are assumed random. Thus, s represents the ratio of RCS of the single scatterer to that of the Rayleigh component. This is often called a "single predominant scatterer" model, although we do not require that s be greater than unity.

The chi-square distributions have been observed empirically to give a good fit to the RCS distributions of many types of targets. However,

except for k=1, there is no theoretical scattering mechanism which exactly gives rise to chi-square distributions.* We previously noted, however, that the chi-square distributions for $k > 1$ are good approximations to Rice distributions; thus, the chi-square distributions can be theoretically explained by a single-predominant plus Rayleigh model. The chief reasons for consideration of the chi-square family are that a) probability of detection curves are available and easily calculated for the complete chi-square family (both strict sense and wide sense), and b) some chi-square cases of interest have empirically been found to correspond to $k < 1$ (Ref. 7) which does not correspond to any Rice distribution.

2.0 Physical Models for Log-Normal Distributions

A log-normal distribution theoretically arises from a product of statistically independent random variables in the limit as the number of factors increases. The difficulty in explaining log-normal amplitude statistics of radar targets on this basis lies in the difficulty of identifying a product of independent or approximately independent random variables with radar targets. Further progress along these lines has been made since these lectures were originally delivered. The results to be stated are due to Drs. R. L. Mitchell and G. E. Pollon.

A first step in the direction of understanding the scattering mechanisms underlying approximately log-normal amplitude statistics is the observation that the amplitude distribution of the gain patterns of directive antennas, viewed at randomly chosen aspects, tends to be approximately log-normal. This has been noticed by deriving empirical distribution functions for such gain patterns. This also suggests that the radar cross section patterns of highly directive scatterers such as flat plates viewed at random aspects may give rise to log-normal RCS statistics, approximately.**

---

*Mathematically, a chi-square distribution with 2k degrees of freedom, 2 k an integer, results from the sum of squares of 2k independent variates drawn from a common Gaussian distribution. For $k \neq 1$, one cannot exactly identify a physical scattering mechanism with such a sum of squares.

**R.L. Mitchell, "Radar Cross Section Statistics of Randomly Oriented Discs and Rods," TSC Project Memorandum 014-10, 26 November 1968.

An illustration of this is shown in Fig. 1 , which shows the empirically-derived cross section statistics of a flat circular plate.* This was computed on the basis of a formula of Siegel et al (Ref. 15, p. 75, Eq. 4.7.5). It is recognized that this formula is an approximation which is poor for small values of D/λ where D = plate diameter, λ = wavelength. However, it is sufficient to illustrate that directive patterns tend to give rise to log-normal RCS statistics. In Fig. 1, the straight line is an exact log-normal distribution with $\sigma = 13$ expressed in db units. Expressed in terms of natural log units, we would have $\sigma = 13/4.34 = 3.0$. Other illustrations could be given for directive scattering mechanisms other than flat plates.

At the time the lectures were originally delivered, it was stated that this is still an empirical rather than a theoretical model for log-normal statistics. Since that time, Dr. Gerald Pollon has developed an approach to the formulation of a theoretical explanation of why sufficientiy directive scatterers give rise to approximate log-normal statistics. This approach succeeds in identifying the RCS of directive scatterers with a product of approximately independent random variables. Thus, this approach results in a theoretical model to explain why directive scatterers give rise to such statistics. This method also is able to yield quantitative, albeit approximate, values for the parameters of such distributions.

A great deal of further work remains to be done relative to physical scattering mechanisms underlying targets whose RCS statistics are observed to be log-normal. For example, in many cases it is observed that the RCS statistics are well approximated by a log-normal distribution which has a σ of considerably less than 3 in natural log units; typically, σ may be say $\sqrt{2}$ or 2. This could not be explained on this basis of single flat plates viewed at completely random aspects. Some additional avenues of investigation would include:

---

*A factor of two error in labelling the curves has been corrected.

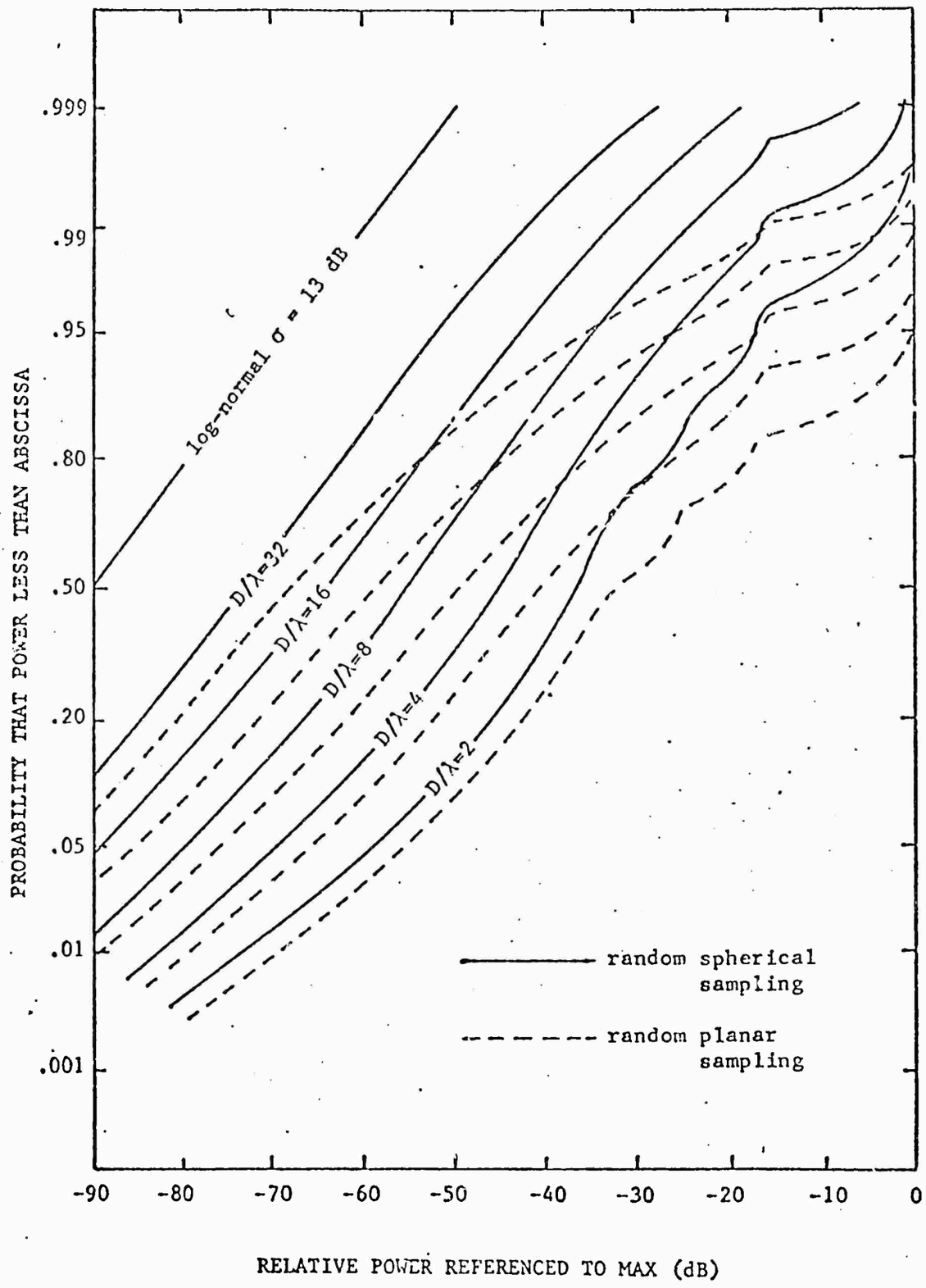

Figure 1. RCS Distribution of a Randomly Oriented Circular Plate

a) RCS statistics of directive scatterers viewed over aspects selected at random from more restricted intervals of aspects (according to Pollon's model, this can result in smaller values of σ.

b) RCS statistics for the phasor sum of several directive scatterers

c) RCS statistics for the phasor sum of directive scatterer and a Rayleigh mechanism (which might be called a single-predominant scatterer mechanism but with a directive predominant scatterer).

It may also be noted that actual scattering patterns have a finite peak value and hence the RCS statistical distribution cannot be exactly log-normal. Possibly truncated log-normal statistics will give a better fit to some observed distributions.

3.0 Various Ways of Utilizing Target Models

The discussion in the two previous sections has emphasized the formulation of closed-form expressions for statistical target models, and has implicitly or explicitly considered that such models will be utilized in calculations of detection probability using closed-form mathematical analysis.

An alternative method of employing target models is to employ them for purposes of Monte Carlo simulation of radar performance. In such an approach, the models might be used to generate many sample functions of dynamic signatures, which in turn would be fed into simulation programs of radar performance.

The use of target models for simulation (as opposed to closed-form calculation) is a primary mode in which target models can be utilized for purposes of analyzing target recognition and identification performance. However, even for detection analysis, there are cases in which the analysis must be done by simulation rather than calculation.

Such situations may arise because:

a) The noise environment is so complicated that closed-form calculation is no longer feasible (e.g., the noise is non-Gaussian, as in certain types of clutter or jamming).

b) The radar receiver involves processes which cannot easily be analyzed in closed form (e.g., certain CFAR techniques).

c) Both of the above may apply.

The target models we have been describing are a convenient basis for generation of statistical sample functions. Each of the three basic families of distribution can be expressed as functions of Gaussian variables u_i. Thus, it is easy to generate a series of correlated samples having Chi-square, Rice, or log-normal amplitude statistics. The steps are:

a) Generate sequences of Gaussian variables having prescribed correlation properties (convenient computer routines exist for this purpose).

b) Carry out the necessary transformations to convert such variables into correlated sequences of Chi-squared, Ri e, or log-normally distributed samples.

c) The values of k, $\bar{x}$, σ, α, s, as well as the parameters governing correlation properties, can also be made programmable to account for changes in the fluctuation distributions as the target moves through the radar surveillance volume.

APPENDIX C

USE OF THEORETICAL SCATTERING MECHANISMS IN MODEL POSTULATION: EXAMPLES

1. Introduction

Theoretical scattering mechanisms associated with various kinds of RCS statistics are useful in postulating consistent models when measured data, or exact physical descriptions, are fragmentary, or in extrapolating models in a consistent manner in such conditions. Lack of knowledge of possible mechanisms underlying given statistics can be a significant obstacle to such postulation or extrapolation. The following examples are intended to illustrate this.

2. Correlation Properties with Respect to Time

Suppose it is desired to postulate possible correlation properties of a target with respect to time, consistent with given RCS statistics (for example consistent with the information that the RCS statistics are Rayleigh, Rice, or log-normal). We will assume that target aspect changes are the physical source of the RCS fluctuations.

a) Rayleigh

Rayleigh statistics (as applied to RCS, this means exponentially distributed) are consistent with a random-phase many-scatterer mechanism without any predominant scatterer or small set of scatterers.

For a target consisting of a large number of relatively isotropic scatterers in random phase, models of the correlation properties with respect to time may be constructed as follows. We will suppose that it is possible, for the target population of interest, to postulate various spatial distributions of such scatterers and various descriptions of target motion.

Let $P(f)df$ denote the fraction of the total scattering cross section which is due to scatterers having doppler shifts between f and $f + df$ with respect to the radar. $P(f)$ can be determined from a spatial distribution of scatterers and the target-radar motion. We will also suppose that

a) P(f) remains constant during the time period of interest

b) the target is illuminated by a sine wave of frequency f_o, with $f_o >>$ bandwidth of P(f).

If those assumptions are not satisfied, the backscattered signal will in general be a non-stationary random process.* The correlation function of such a non-stationary process can be calculated, but this is beyond the intended scope of this illustration.

Under the stated assumptions; the one-sided power spectrum of the received signal is

$$S(f) = \psi_o \, P(f - f_o) \tag{C-1}$$

where A is a constant chosen such that

$$\int_o^\infty S(f) = \text{total average received power} \tag{C-2}$$

the correlation function $\varphi(t)$ is simply the Fourier cosine transform of S(f):

$$\varphi(t) = \int_o^\infty \cos 2\pi ft \; S(f) \, df \tag{C-3}$$

However, for purposes of determining the target's correlation properties, it is of more interest to know the correlation function of the complex signal envelope, i.e., with the carrier frequency f_o and the mean doppler shift of the target removed. To this end, let

$$\bar{f} = \text{mean doppler shift of target} \tag{C-4}$$

and let the return signal be represented as

$$r(t) = u_1(t) \cos 2\pi(f_o + \bar{f})t - u_2(t) \sin 2\pi(f_o + \bar{f})t \tag{C-5}$$

---

*If assumption (b) is not satisfied, the backscattered signal can still be stationary if the target is very extended and with uniform average density of scatterers Poisson-distributed in time delay. By an extension of Campbell's theorem, the spectrum would be proportional to the convolution of P(f) with $|F(f)|^2$, where F(f) is the Fourier transform of the waveform. However, this is of more interest for clutter models than for target models.

Then

$$E[u_1(t)u_1(t+\tau)] = E[u_2(\tau)u_2(t+\tau)] \qquad \text{(C-6)}$$

$$= \frac{\Psi_o}{2} \text{ Real part of } \int_{-\infty}^{\infty} P(f-\bar{f})e^{2\pi i f\tau}df$$

$$E[u_1(t)u_2(t+\tau)] = - E[u_1(t+\tau)u_2(t)] \qquad \text{(C-7)}$$

$$= \frac{\Psi_o}{2} \text{ Imaginary part of } \int_{-\infty}^{\infty} P(f-\bar{f})e^{2\pi i f\tau}df$$

If a pulse radar illuminates such a target at times t_i, the correlation matrix of the samples $u_{i1} = u_1(t_i)$ and $u_{i2} = u_2(t_i)$ can be determined from (C-6) and (C-7) with $\tau = t_i - t_j$.

b) Rice

For a Rice scattering mechanism, define P(f) for the many-scatterer component* but now define

$$\bar{f} = \text{doppler shift of predominant scatterer} \qquad \text{(C-8)}$$

and then apply eqs. (C-5)-(C-7) to the many-scatterer component. This gives the necessary correlation matrix of u_{i1} and u_{i2}, the sine and cosine components of the many-scatterer component, which in turn suffices to define the whole joint statistics of the RCS samples.

c) Log-Normal

We know that log-normal RCS statistics are not produced by a many-random-phase-scatterer mechanism or by such a mechanism plus a predominant non-fluctuating scatterer. Thus, the postulation of models for correlation properties of such targets requires physical models which would give rise to log-normal RCS statistics.

---

* That is, P(f)df now represents the fraction of the many scatterer component with doppler shifts between f and f+df.

3. Effects of Frequency Diversity

Use of frequency diversity together with pulse integration to smooth out fluctuations is a technique of great potential benefit in modern radar, both for detection and tracking. Thus, it becomes of interest to postulate fluctuation models with respect to the RCS frequency signature. Among the important questions that may be asked for particular target populations are:

a) Does frequency diversity always cause fluctuations of RCS for targets which fluctuate with respect to aspect?

b) Can it be consistently postulated that the fluctuations caused by frequency diversity come from the same statistical distribution as when the fluctuations are due to aspect changes?

c) In general, how should one postulate models of the p.d.f. and correlation properties of target fluctuations with respect to frequency, given the information that the fluctuations with respect to aspect have specified statistical models?

Some illustrations will suffice to show that the answers to questions (a) and (b) may be negative, and that the answer to question (c) may not always be obvious.

An example of a type of target which will fluctuate with respect to aspect changes but will be non-fluctuating with respect to frequency changes is provided by a prolate or oblate spheroid satisfying the condition that for all frequencies under consideration, the radii of curvature are much greater than the wavelength. The RCS of such a target at any aspect is equal to $\pi r_1 r_2$, where r_1 and r_2 are the radii of curvature at the point on the target such that the tangent plane is normal to the line of sight to the radar. Consequently, there will be no fluctuation with frequency (so long as $\lambda \ll r_1$ and $\lambda \ll r_2$). On the other hand, $r_1 r_2$ changes as aspect changes, so that there will be RCS fluctuations with aspect.

A converse example is that of a sphere in the resonance region ($\lambda \approx 2\pi a$); here, there will be RCS fluctuations with respect to frequency but not with respect to aspect.

Turning to the major categories of statistical target model:

a) Rayleigh and Rice

A target which has Rayleigh fluctuations with aspect is consistent with a many-scatterer mechanism which will also fluctuate with respect to frequency, with the samples of RCS also coming from an exponential p.d.f., in fact from the same p.d.f. as the aspect fluctuations.

The correlation properties with respect to frequency will of course be calculated or modelled differently than those with respect to aspect. In fact, to calculate correlation properties with respect to frequency, let $P(u)du$ = fraction of target RCS due to scatterers in the time-delay interval u to $u+du$ (here, $u = 2R/c$, R = range, c = velocity of light).

Then, $P(u)$ plays the same role in the calculations as $P(f)$ played in calculating the correlation properties with respect to time.

For Rice targets, assuming the predominant scatterer is non-fluctuating with frequency (a consistent assumption although not a necessarily true one), the RCS fluctuations with frequency can also be consistently postulated to be drawn from the same Rice distribution as the fluctuations with respect to aspect (i.e., they will have the same p.d.f.), while the correlation properties of the many-scatterer component will be dependent on $P(u)$.*

b) Log-Normal

If a target is observed to have log-normal fluctuation statistics with respect to aspect changes, it would not be clear what statistics could consistently be postulated for fluctuations with respect to frequency unless a physical mechanism for log-normal statistics is known.

Although more work remains to be done, the directive scatterer model for log-normal statistics indicates that it is at least consistent to postulate models for which questions (a) and (b) stated above can be answered affirmatively. This is because of the duality between small frequency changes and small aspect changes on the side lobes of directive scatterers. The directive scatterer model also suggests the method of postulating correlation properties with respect to frequency.

---

*$P(u)$ is now defined just for the many-scatterer component.

c) Rule of Thumb for Uncorrelated Samples

A convenient rule of thumb for approximately uncorrelated samples, with respect to either frequency or aspect diversity, applicable at least to many-scatterer targets or to the many-scatterer component of Rice targets, is as follows: samples will be approximately uncorrelated if the range difference for at least some pairs of scatterers has changed by at least 1/2 of a wavelength unit one-way (the change may be due either to a range-difference change for fixed λ or to a change in λ).

When applied to frequency diversity, this implies that the frequency increment required for uncorrelated samples is

$$\Delta f \approx \frac{c}{2\delta R} \tag{C-9}$$

where

δR = range extent of significant scattering centers if the latter is smaller than the radar range resolution

δR = radar range resolution if the latter is smaller than the range extent of target scattering centers.

4. Models for Range-Extended Targets

With increasing range resolution capabilities of modern radars, it becomes of interest to conduct detection analyses for targets whose electromagnetic range extent exceeds the range resolution cell width. Such analyses are aimed not only at predicting performance for specific designs but also at questions such as a) how small should the resolution cell be made to optimize detection performance, or b) how should signals in contiguous range cells be processed to optimize detection performance? These questions become especially pertinent in clutter-dominant situations, where decreasing the resolution cell size decreases the average clutter power.

In performing detection analyses in such cases it becomes clear that a generalized type of target model is required. Specifically, the target model must describe the statistical fluctuation properties of those portions of the target in each resolution cell, and how such fluctuation properties change as the cell size is varied.

Since actual data, on which such models can be based, are rather scarce, it is of interest to consider the question of postulating such models in such a way as to be consistent. Illustrations follow.

a) Rayleigh Targets

Suppose it is known or assumed that a certain population of targets have Rayleigh fluctuation statistics when the resolution cell size equals or exceeds the target electromagnetic extent. In this case, it is simple to postulate consistent models for smaller resolution cells. Rayleigh statistics for the target as a whole are consistent with the following models (for example):

(i) A model in which the portion of the target in each resolution cell is also a Rayleigh target (i.e., a many-scatterer mechanism).

(ii) A model in which the portion of the target in some or all cells are Rice or chi-square targets when the cells become small.

(iii) A model in which, for sufficiently small cell size, the portion of the target in each cell is non-fluctuating.

In any of these cases, it would be consistent to postulate that the rate of fluctuation of the contents of each range cell is less than or equal to the rate of fluctuation for larger cells.

b) Rice Targets

If the target as a whole is known to have Rice fluctuation statistics, consistent models could be postulated similar to those stated above, except that at least one cell would always contain a Rice target. Moreover, the ratio of predominant to Rayleigh components in that cell would increase with decreasing cell size.

c) Log-Normal Targets

Suppose the whole target has log-normal RCS statistics. The question of how to model the target fluctuation properties when the resolution cell becomes smaller than the target in such cases requires further investigation. The directive scatterer model for log-normal statistics indicates an approach, but the problem remains to be solved.

REFERENCES FOR APPENDICES B AND C

1. J. I. Marcum and P. Swerling, "Studies of Target Detection by Pulsed Radar," IRE Trans. Info. Theory, Vol. IT-6, No. 2, April 1960.

2. P. Swerling, "Probability of Detection for Some Additional Fluctuating Target Cases," Aerospace Corp. Report No. TOR-669(9990)-14, March 1966.

3. G. R. Heidbreder and R. L. Mitchell, "Detection Probabilities for Log-Normally Distributed Signals," IEEE Trans. on Aerospace and Electronic Systems, Vol. AES-3, No. 1, January 1967; also Aerospace Corp. Report No. TR-669(9990)-6, April 1966.

4. P. H. R. Scholefield, "Statistical Aspects of Ideal Radar Targets," IEEE Proceedings, Vol. 55, No. 4, April 1967.

5. S. O. Rice, "Mathematical Analysis of Random Noise," in Wax, N., Noise and Stochastic Processes, Dover, 1954.

6. R. W. Kennedy, "The Spatial and Spectral Characteristics of the Radar Cross Section of Satellite-Type Targets," Air Force Avionics Laboratory, Wright-Patterson Air Force Base, Tech. Report AFAL-TR-66-17, March 1966.

7. W. W. Weinstock, "Target Cross Section Models for Radar Systems Analysis," Ph.D. Dissertation, University of Pennsylvania, Philadelphia, Pa., 1956.

8. P. Swerling, "More on Detection of Fluctuating Targets," IEEE Trans. Info. Theory, Vol. IT-11, No. 3, July 1965.

9. P. Swerling, "Detection of Fluctuating Pulsed Signals in the Presence of Noise," IRE Trans. Info. Theory, Vol. IT-3, No. 3, September 1957.

10. G. A. Campbell and R. M. Foster, "Fourier Integrals for Practical Applications," D. Van Nostrand, New York, 1947.

11. L. F. Fehlner, "Marcum's and Swerling's Data on Target Detection by a Pulsed Radar," Applied Physics Laboratory, Johns Hopkins University, TG-451, 2 July 1962.

12. L. E. Brennan and I. S. Reed, "A Recursive Method of Computing the Q-function," IEEE Trans. Info. Theory, Vol. IT-11, No. 2, April 1965.

13. P. Swerling, "Detection of Radar Echoes in Noise Revisited," IEEE Trans. Info. Theory, Vol. IT-12, No. 3, July 1966.

14. P. Swerling, "Maximum Angular Accuracy of a Pulsed Search Radar," IRE Proceedings, Vol. 44, No. 9, September 1956.

REFERENCES (Continued)

15. J. W. Crispin, R. F. Goodrich, and K. M. Siegel, "A Theoretical Method for the Calculation of the Radar Cross Sections of Aircraft and Missiles," University of Michigan Report No. 2591-1-H, July 1959.

16. P. Swerling, "Comments on Statistics of Fluctuating Target Detection," IEEE Trans. Aerospace and Electronic Systems (Correspondence), Vol. AES-2, No. 5, September 1966, pp. 621-622.

17. M. Abramovitz and I. A. Stegun, Handbook of Mathematical Functions, Applied Math. Series 55, National Bureau of Standards, Washington, D. C., June 1954.

18. A. M. Mood, Introduction to the Theory of Statistics, McGraw-Hill Book Co., New York, 1950.

19. R. R. Boothe, "A Digital Computer Program for Determining the Performance of an Acquisition Radar Through Application of Radar Detection Probability Theory," U.S. Army Missile Command Report RD-TR-64-2, December 1964.

20. Proc. IEEE, Radar Reflectivity Issue, Vol. 53, No. 8, August 1965.